In vitro endoderm emergence and self-organisation in the absence of extraembryonic tissues and embryonic architecture

Stefano Vianello[1] ✉ **and Matthias Lutolf**[1,2] ✉

[1]Laboratory of Stem Cell Bioengineering, Institute of Bioengineering, School of Life Sciences (SV) and School of Engineering (STI), Ecole Polytechnique Fédérale de Lausanne (EPFL), Lausanne, Switzerland
[2]Institute of Chemical Sciences and Engineering, School of Basic Science (SB), EPFL, Lausanne, Switzerland

The endoderm is the cell lineage which gives rise in the embryo to the organs of the respiratory and gastrointestinal system. In the mouse this may be the germ layer with the strongest association with its extraembryonic counterpart. Uniquely indeed, endodermal tissue does not just derive from descendants of the embryo proper (the epiblast) but instead arises from their gradual incorporation into an extraembryonic substrate (the visceral endoderm). Given the configuration of the early embryo, such a paradigm requires epiblast endodermal progenitors to negotiate embryonic compartments with very diverse epithelial character, a developmental contingency reflected by the fact that key early endodermal markers such as *Foxa2* and *Sox17* have been consistently found to be embedded within gene programmes involved in epithelialisation.

To explore the underlying cell biology of embryonic endoderm precursors, and to explore the relationship between endoderm development, epithelial identity, and extraembryonic mixing, we leveraged Gastruloids, *in vitro* models of early development. These self-organising three-dimensional aggregates of mouse embryonic stem cells do not possess an extraembryonic component, nor do they appear to display typical tissue architecture. Yet, they generate cells expressing endodermal markers. By tracking these cells throughout *in vitro* development, we highlight a persistent and uninterrupted pairing between epithelial and endodermal identity, with FoxA2+/Sox17+ endoderm progenitors never transitioning through mesenchymal intermediates and never leaving the epithelial compartment in which they arise. We also document the dramatic morphogenesis of these progenitors into a macroscopic epithelial primordium extending along the entire anterior-posterior axis of the Gastruloid, patterned into broad domains of gene expression. Corollarily we thus also reveal an underappreciated epithelial component in Gastruloids, and thus the spontaneous emergence *in vitro* of stratified architectures and germ layer compartmentalisation.

gastruloid | endoderm development | epithelium | self-organisation
Correspondence: ***stefano.vianello@epfl.ch and matthias.lutolf@epfl.ch***

Introduction

In mouse and humans, the digestive track, the respiratory system, and key internal organs such as the thyroid, the bladder, the pancreas and the liver all derive from the same progenitor tissue (Carlson, 2014; Lewis & Tam, 2006; Nowotschin et al., 2019a), a "mucous layer" first described in chick embryos (Pander, 1817), and which we now know as "endoderm" (Allman, 1854; Oppenheimer, 1940).

In mouse, this "inner skin" actually first assembles on the outer surface of the embryo, through a unique choreography of cellular movements illustrated in Figure 1 (Burtscher & Lickert, 2009; Kwon et al., 2008; Viotti et al., 2014). As the mouse embryo implants into the uterus of the mother, and extraembryonic tissues proliferate to impart to the conceptus its characteristic cylindrical shape (Smith, 1985), the mouse embryo (at the very tip of such cylinder) is little more than an epithelial mass of potent cells: the epiblast. Remarkably, such inconspicuous tissue will act as the origin of almost all cells of the developing embryo, and this by engaging a complex series of biological, mechanical, and topological transformations coupling proliferation to cell fate restriction and cell rearrangement. Such a complex series of transformations, gastrulation, is a key milestone of all embryonic development. As such, the initially multipotent and uncommitted cells of the early epiblast commit to specific fates, which are generally classified into the broad germ layer categories of ectoderm (skin and neural types), mesoderm (heart, muscles, and mesenchyme), and endoderm (internal organs, respiratory and digestive tract) (Arnold & Robertson, 2009; Takaoka & Hamada, 2012; Tam & Behringer, 1997; Tam & Loebel, 2007).

Yet we now know that at least one of these germ layers, the endoderm, does not come entirely from cells originating in the epiblast (Kwon et al., 2008; Nowotschin et al., 2019a,b; Viotti et al., 2014). Blurring the boundaries of prevalent developmental paradigms, and making such qualifiers somehow oxymoronic, "extraembryonic" cells (i.e. cells that segregated away from the epiblast early on even before implantation) also contribute to the embryo, and specifically to its endoderm-derived tissues. Indeed, the epiblast is not isolated from other tissues within the conceptus, and it is actually enveloped by a thin epithelium of so-called Visceral Endoderm (Figure 1A, in yellow). This latter sheet of cells on the surface of the epiblast is what one would classify as extraembryonic tissue, originating from much earlier lineage

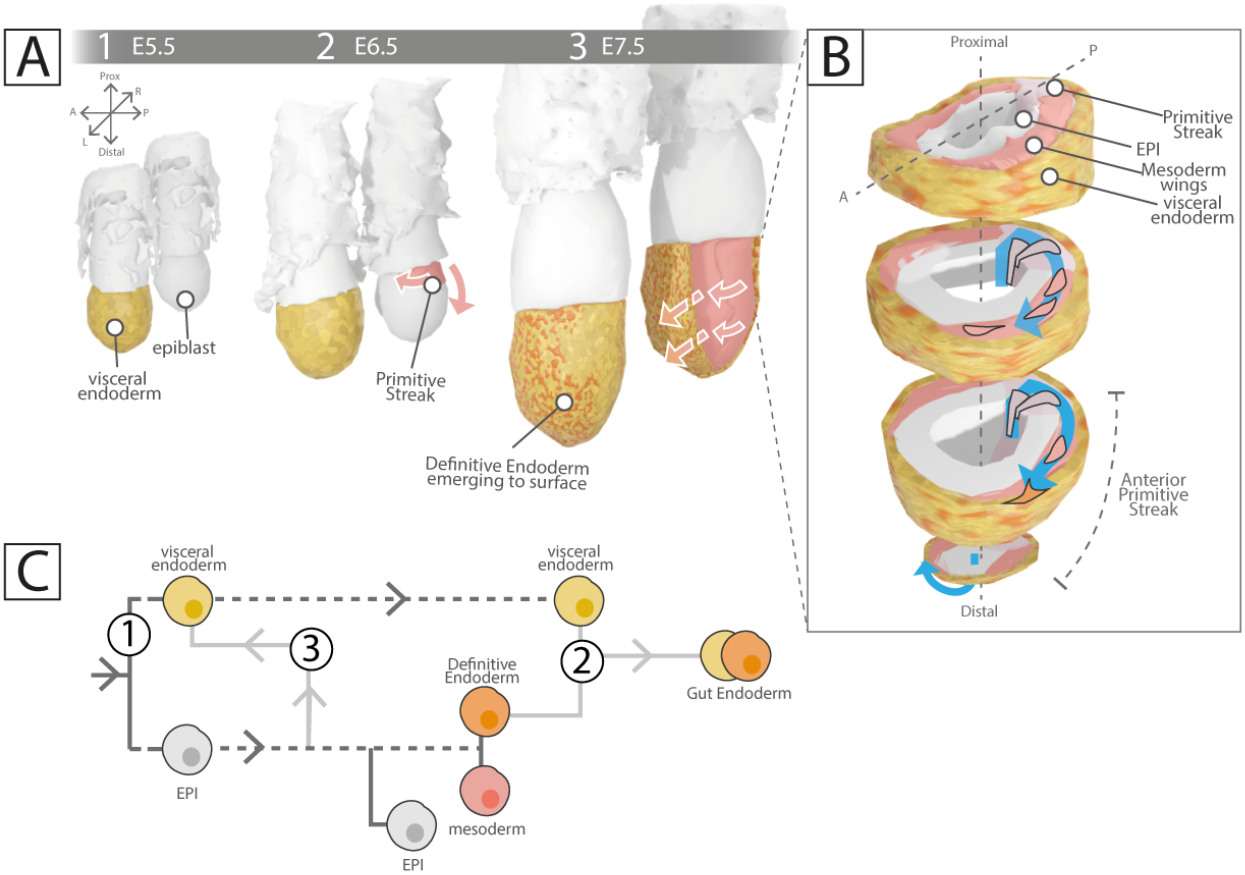

Fig. 1. Endoderm development in the mouse embryo. (**A**) Intercalation of (embryonic) definitive endoderm cells (orange) into the visceral endoderm epithelium (yellow, extraembryonic), during peri-gastrulation stages of mouse development. In red, mesodermal cells emerging from the primitive streak and starting their posterior-to-anterior circumnavigation of the epiblast. (**B**) Exploded view of the mouse embryo at around E7.5, as if sectioned proximo-distally. At the posterior of the epiblast a zone of EMT (primitive streak, light purple) advancing towards the disal tip of the embryo mediates epiblast cell egression. Cells specified to mesoderm (red cells) leave the epiblast and form so-called mesodermal wings as they circumnavigate the epiblast. They are sandwiched between the epiblast they just left (gray), and the overlaying visceral endoderm (yellow). Defintive endoderm cells (orange) transit only shortly within the mesodermal compartment, and instead egress into the visceral endoderm. (**C**) The multiple origins of endodermal cells, as adapted from (Nowotschin et al., 2019b). 1) visceral endoderm cells, originating from earlier segregation between "embryonic" and "extraembryonic" cell types in the blastocyst, 2) intermixing with definitive endoderm cells arising from gastrulation (see previous panels), 3) direct delamination from the epiblast prior to gastrulation. E = embryonic day.

segregation events (Chazaud et al., 2006). Originally thought to be displaced away as the embryo develops, this thin sheet of "extraembryonic" cells is the primary destination of a subset of cells produced by the epiblast (i.e. embryonic cells, in orange throughout Figure 1A), that these embryonic cells are those that will make endoderm, and as such that the visceral endoderm "extraembryonic" sheet in which these cells intercalate becomes itself an integrated component of later embryonic structures (Burtscher & Lickert, 2009; Kwon et al., 2008; Nowotschin et al., 2019b; Viotti et al., 2014).

How does this process start? At around embryonic day (E)6.25 asymmetric signalling by extraembryonic tissues surrounding the epiblast break its symmetry (Stower & Srinivas, 2018; Takaoka & Hamada, 2012). One side of the epiblast starts becoming different from the rest (Figure 1A.2). At this side, which is defined as the posterior of the embryo and at which extraembryonic tissues concentrated high Wnt, BMP, and FGF signalling activity, epiblast cells respond by engaging so-called Epithelial to Mesenchymal Transition (EMT) programmes: they start losing attachment with the rest of the epithelium, they become motile and mesenchymal, they leave the epiblast (Arnold & Robertson, 2009; Tam & Behringer, 1997; Tam & Loebel, 2007). Morphologically, the so-called Primitive Streak appears: a distally-expanding zone of EMT leading to delamination of epiblast cells and simultaneous commitment to embryonic fates (Hashimoto & Nakatsuji, 1989; Williams et al., 2011). As epiblast cells undergo EMT and leave the epiblast, they start circumnavigating its outer surface, sandwiched under the overlaying visceral endoderm, forming wings of tissue converging towards the anterior of the embryo ((Hashimoto & Nakatsuji, 1989; Viotti et al., 2014); red intervening intervening tissue in Figure 1A.2 and 1A.3, and red cell trajectory in Figure 1B). These cells will generate mesodermal derivatives, heart and muscles (Tam & Behringer, 1997).

Within the mesodermal compartment of the embryo another cell type finds its way: endodermal cells. Like mesodermal cells, these cells were once epiblast cells that left that epithelium to egress into the mesodermal compartment (Burtscher & Lickert, 2009). Rather than remaining within these wings of mesoderm however, endodermal cells start establishing contacts with the overlaying epithelium, the visceral endoderm, into which they eventually integrate (orange cell in Figure 11B; (Burtscher & Lickert, 2009; Kwon et al., 2008; Viotti et al., 2014)). The outer surface of the embryo thus quickly becomes a mosaic of its original resident population, that of visceral endoderm cells, and of an increasing number of ingressing and intercalating endoderm cells of embryonic (epiblast) origin, so-called Definitive Endoderm cells ((Burtscher & Lickert, 2009; Kwon et al., 2008; Viotti et al., 2014); orange cells in Figure 1A.3). This sheet of cells will later form pockets at the anterior and posterior of the embryo, and finally fold along its midline to close into a tube that will end up internalised within the embryo (not illustrated; (Carlson, 2014; Lewis & Tam, 2006; McGrath & Wells, 2015)). The gut tube has formed, and along its entire length progenitors of all endoderm-derived visceral organs will emerge and take shape (Carlson, 2014; McGrath & Wells, 2015).

Clearly then, what ultimately becomes the tissue we refer to as "gut endoderm", i.e. the endodermal sheet which folds and closes to give rise to the embryonic gut tube, is thus actually a mixture of cells of very different origins, even though these converge towards similar (yet not identical) endpoint molecular signatures (Nowotschin et al., 2019a,b; Viotti et al., 2014). The multiple contributions to gut endoderm described above are summarised in Figure 1C (as adapted from e.g. (Nowotschin et al., 2019a)). In addition to the first contribution of Visceral Endoderm cells by early segregation within the inner cell mass of the early embryo (Figure 1C.1), and to the later intercalation of Defintive Endodem cells (Figure 1C.2), we also highlight a third source of cells: epiblast cells bypassing EMT and altogether bypassing transit within the mesodermal compartment of the embryo. These cells leave the epiblast to directly intercalate into the visceral endoderm, a contribution that has been documented to occur at the distal tip of the pre-gastrulation mouse embryo, zone of maximal mechanical stress (Hiramatsu et al., 2013; Matsuo & Hiramatsu, 2017), and that has found confirmation from single-cell transcriptome analyses (Nowotschin et al., 2019b). Direct epiblast to endoderm transitions are particularly interesting, as even endodermal progenitors that do classically egress from the epiblast into the mesodermal space seem to do so by EMT processes different than those governing the egression and specification of mesoderm (Bardot & Hadjantonakis, 2020; Burtscher & Lickert, 2009). As such, egressing endodermal progenitors do not completely lose their epithelial character but instead transiently redistribute their surface adhesion molecules as they travel along the mesodermal compartment, until they contact their new epithelial niche, the visceral endoderm, and fully repolarise (Bardot & Hadjantonakis, 2020; Kwon et al., 2008; Nowotschin et al., 2019a; Viotti et al., 2014).

Uncertainty remains regarding the exact nature of the transition states that embryonic endoderm precursors traverse as they leave epiblast potency and refine endodermal identity (Bardot & Hadjantonakis, 2020; Lewis & Tam, 2006). Notably, evidence for so-called "mesendodermal progenitors", whereby bipotential cells able to give rise to both mesoderm and endoderm would exist within or outside the epiblast, is debated in mouse (Lewis & Tam, 2006) despite the clear existence of such progenitor state in other developmental models (e.g. sea urchin and roundworms; (Peter & Davidson, 2010; Sulston et al., 1983)). Certainly, segregation between the two germ layers in the mouse is documented already at very early stages, and actually within the very pre-streak epiblast (Burtscher & Lickert, 2009). Uncertainty also remains on whether endodermal cells egress from the epiblast through mechanisms common to those of egressing mesodermal cells or through alternative mechanisms. Crucially, the observation that endodermal cells can be seen to have left the epiblast in regions which the primitive streak has not yet reached (Burtscher & Lickert, 2009), and that those within mesoderm wings of the embryo have not lost their epithelial identity (Viotti et al., 2014) raise interest in the relationship between epitheliality and endodermal identity (Viotti et al., 2014). Given the recent spotlight on the mixed composition and distribution of gut endoderm cells (Nowotschin et al., 2019b), one also wonders whether extraembryonic and embryonic endoderm cells play distinct essential roles within this primordium and its derivatives. In embryos where embryonic endoderm precursors cannot integrate their extraembryonic substrate and remain trapped within the mesodermal compartment, these lose their identity and embryos do not form midgut and hindgut (Kanai-Azuma et al., 2002; Viotti et al., 2014).

As a platform to explore the underlying cell biology of embryonic endoderm precursors, and to explore the relationship between endoderm development, epithelial identity, and extraembryonic mixing, we use Gastruloids (Beccari et al., 2018; Turner et al., 2017; van den Brink et al., 2014). These stem cell aggregates develop *in vitro* in times and patterns that are surprisingly but consistently reminiscent of *in vivo* embryonic development. While mainly characterised in terms of mesodermal and neuromesodermal development (van den Brink et al., 2020), they have been crucially also found to specify endodermal identities ((Beccari et al., 2018; Pour et al., 2019; Turner et al., 2017; van den Brink et al., 2014; Veenvliet et al., 2020); see also Discussion). Work with this system reflects a paradigm whereby leaving cells to their own self-organisation exposes intrinsic cellular programmes and developmental modules that would be otherwise masked by the regulative context of normal embryonic development (Davies, 2017; Shahbazi & Zernicka-Goetz, 2018; Turner et al.,

2016). In this perspective, the absence of typical embryonic architecture, compartmentalisation, and extraembryonic tissues, makes Gastruloids particularly suitable to study the relevance of these features to endoderm development.

We here highlight a persistent and uninterrupted pairing between epithelial and endodermal identity, with FoxA2+/Sox17+ endoderm progenitors never transitioning through mesenchymal intermediates and never leaving the epithelial compartment in which they arise. We also document the dramatic morphogenesis of these progenitors into a macroscopic epithelial primordium extending along the entire anterior-posterior axis of the Gastruloid, patterned into broad domains of gene expression. Corollarily we thus also reveal an underappreciated epithelial component in Gastruloids, and thus the spontaneous emergence *in vitro* of stratified architectures and germ layer compartmentalisation.

Results

To investigate the emergence, dynamics, and patterning of endoderm progenitors *in vitro* we started by generating Gastruloids (Baillie-Johnson et al., 2015; Beccari et al., 2018; van den Brink et al., 2014). Accordingly, we aggregated 300 mouse embryonic stem cells of a TBra/Sox1 double reporter line (described in (Deluz et al., 2016)) whose output Gastruloids have been extensively characterised in published literature and for which we have documented expression of markers of all three germ layers ((Beccari et al., 2018)); see Materials & Methods). As expected, when 300 of these mouse embryonic stem cells are seeded in individual wells of a low-adhesion 96well plate and maintained in N2B27 medium, these sediment to the bottom of the well and aggregate together in the first 48h of culture to form a compact sphere with defined edges by 72h (Figure 2). A pulse of the glycogen synthase kinase (GSK) 3 inhibitor (CHIR99021, Chiron) is then applied as a trigger of "gastrulation" and as to mimic the increase in Wnt signalling experienced by cells of the posterior mouse epiblast. Accordingly, the aggregate breaks symmetry (Figure 2A, asterisk). Morphologically, the spherical 72h aggregate becomes oblong by 96h, and extends a long protrusion that grows over time (120h, 144h). This posterior protrusion is marked by *TBra* (Brachyury) expression, marker of the posterior primitive streak and of the embryonic tail bud, and found to similarly define the posterior of the Gastruloid (Beccari et al., 2018; Turner et al., 2017; van den Brink et al., 2014).

Emergence and patterning of endodermal markers.

Emergence of early endodermal markers. In the embryo, precursors of the definitive endoderm can be found within epiblast cells marked by expression of the transcription factor FOXA2 (Burtscher & Lickert, 2009). These FOXA2+ cells are initially intermingled with TBra+ (TBXT) cells at the proximal posterior side of the embryo, and then resolve as a homogeneous FOXA2+ population marking the distal portion of the epiblast, and thus the epiblast region anterior to the leading edge of the primitive streak (Bardot et al., 2017; Burtscher & Lickert, 2009). While cells in the intervening epiblast region and co-expressing *FoxA2* and *TBra* may be progenitors of cardiac mesoderm types (Bardot et al., 2017), FOXA2+ cells of the distal epiblast are posited to leave the columnar epithelium, upregulate *FoxA2*, and move within the wings of mesoderm enveloping the epiblast ((Burtscher & Lickert, 2009; Kwon et al., 2008; Viotti et al., 2014), see also Figure 1B). FOXA2+ cells that contact the overlaying visceral endoderm upregulate *Sox17* (Viotti et al., 2014), leave the mesodermal domain, integrate within this new epithelium, and join the cohort of cells that will eventually form the gut endoderm (Burtscher & Lickert, 2009; Kwon et al., 2008; Viotti et al., 2014). Given the relevance of *FoxA2* and *Sox17* for endoderm development (Dufort et al., 1998; Kanai-Azuma et al., 2002; Monaghan et al., 1993; Sasaki & Hogan, 1993), and their prevalent use in the gastruloid/embryoid literature as early endoderm markers (Beccari et al., 2018; Pour et al., 2019; Turner et al., 2017; van den Brink et al., 2014; Veenvliet et al., 2020), we decided to track their emergence and patterns of expression at the earliest stages of Gastruloid development.

At 72h, when the Gastruloid is still spherical and has just received the CHIR stimulus that will drive it through differentiation and morphogenesis, FOXA2+ cells can be seen scattered throughout the aggregate, intermingled with TBra+ cells (Figure 2B.1, 72h). Just 24h later (t=96h), and as TBra+ cells resolve into a pole that will accordingly define the posterior of the Gastruloid (van den Brink et al., 2014), FOXA2+ cells form clusters and segregate away from the TBra+ pole along the newly defined axis of the aggregate (Figure 2B.1, 96h) . While few FOXA2+/TBra+ (double-positive) cells can be distinguished at this stage, most cells are either TBra+ at the posterior of the Gastruloid, or FOXA2+ as scattered clusters along the anterior (Figure 2B.1,bottom).

In contrast to TBra and FOXA2, SOX17 cannot be detected at t=72h, but only starts appearing later (Figure 2B.2). At t=96h, scattered unclustered SOX17+ cells appear within the elongating Gastruloid, and co-staining for FOXA2 shows these cells as representing a nearly exclusive subset of the FOXA2+ population (Figure 2B.3). We thus observe, at the earliest timepoints of Gastruloid response to CHIR, ordered emergence of key endodermal markers in sequence and patterns that are consistent with what is observed in the embryo. Not only SOX17+ cells emerge later and within a population of FOXA2+ cells (Viotti et al., 2014), these cells sort from an initially TBra-intermingled population to later define posterior and anterior domains along the AP axis of the Gastruloid, just as is observed in the epiblast of the early primitive streak embryo (Burtscher & Lickert, 2009).

Cellular biology of endodermal cells. In vivo, FoxA2+ (and thus Sox17+) cells are expected to occupy and traverse very different embryonic compartments throughout their journey.As such, FOXA2+ cells will first emerge within the columnar epithelial tissue of the epiblast, they will

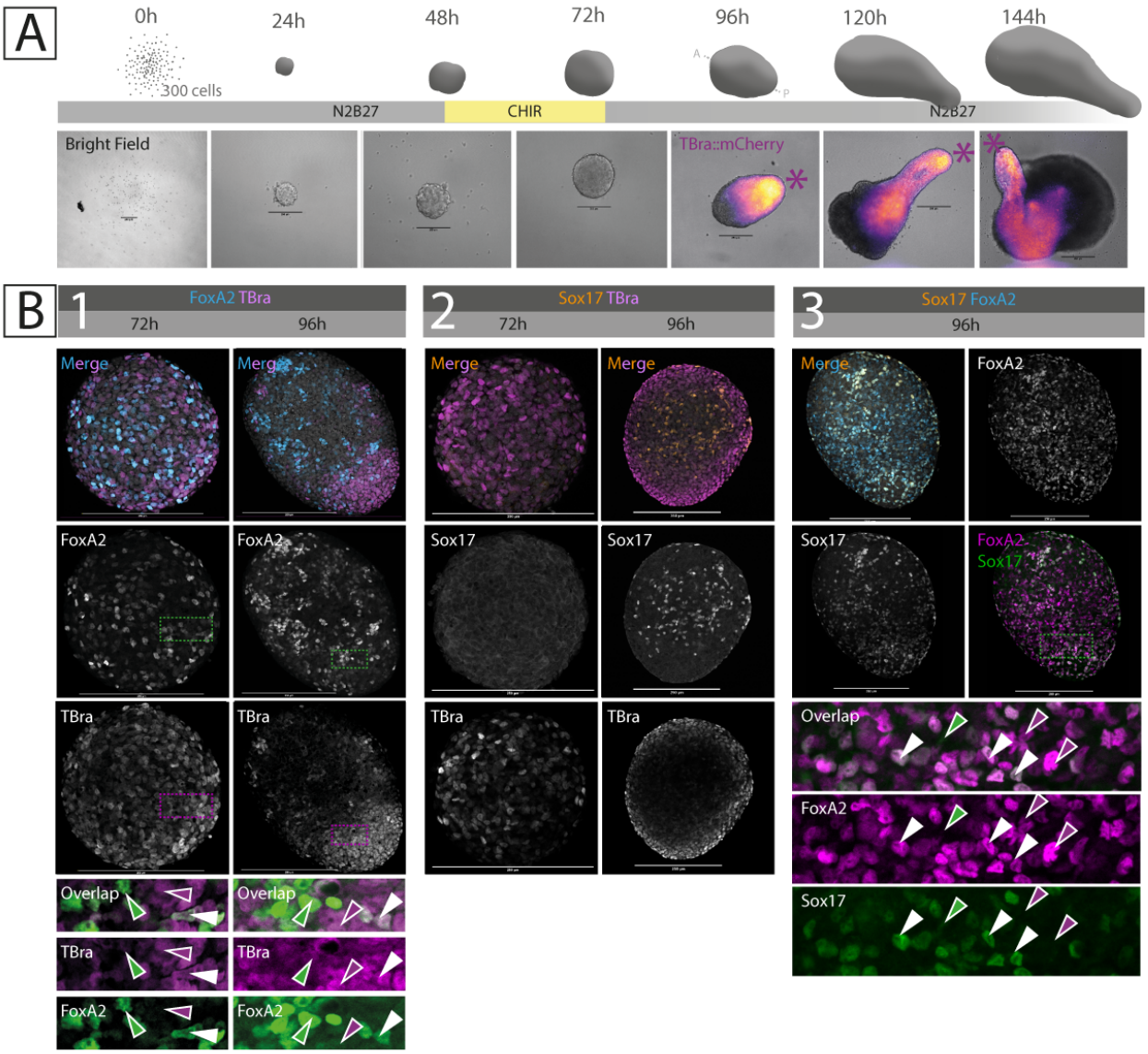

Fig. 2. Emergence and patterning of endodermal markers in Gastruloids. (**A**) Summary schematic of the Gastruloid generation protocol (see Methods), and brightfield pictures of representative Gastruloids all along their development *in vitro*. Note that the fluorescence channel is here shown from t=96h onward only (when the Gastruloid becomes polarised). Reporter expression starts at t=72h, homogeneously throughout the spheroid (see (Turner et al., 2017)). (**B**) Immunostaining against the posterior epiblast and primitive streak marker TBra, and classical endodermal progenitor markers FoxA2 and Sox17, at 72h and 96h of Gastruloid development. SOX17+ cells appear one day later TBra+ and FOXA2+ cells, and are a nearly exclusive subset of the latter. Marker colocalisation is shown in green and magenta, with double-positive cells appearing white (examples of single-positive and double-positive cells highlighted by single-colour and white arrowheads respectively). Scale bar is always 250um. Asterisk indicates the posterior of the Gastruloid (based on TBra expression).

then egress and mix with the mesenchymal mesodermal cell types circumnavigating the embryo as mesodermal wings, and they will finally re-integrate the epithelium on the surface of the embryo ((Kwon et al., 2008; Viotti et al., 2014), as illustrated in Figure 1B). Sox17 expression appears to be even more intimately associated with transitions between compartments, and expressed once endodermal precursors contact and integrate within the surface epithelium (Viotti et al., 2014). We thus sought to resolve whether cells expressing endodermal markers in Gastruloids were equivalently moving across compartments, with particular attention to their epithelial identity. Indeed, we observe SOX17+ cells in the absence of surface epithelial layer on which these would eventually integrate *in vivo*.

Co-staining for the the epithelial marker CDH1 (E-cadherin, adherens junction) shows that both TBra+ and FOXA2+ cells specified within the t=72h Gastruloid are emerging within a cellular aggregate that is uniformly epithelial (or, at least, epithelioid, Figure 3A), consistently with the epithelial context of the epiblast of the early gastrulation embryo in which TBRA+ and FOXA2+ cells first arise (Burtscher & Lickert, 2009). Cells of the t=72h Gastruloid all show homogeneous membrane CDH1 localisation, as likely expected for an aggregate of embryonic stem cells transitioning towards EpiSC states (Hamidi et al., 2020; Turner et al., 2017).

Interestingly, the CDH1 landscape of the t=96h Gastru-

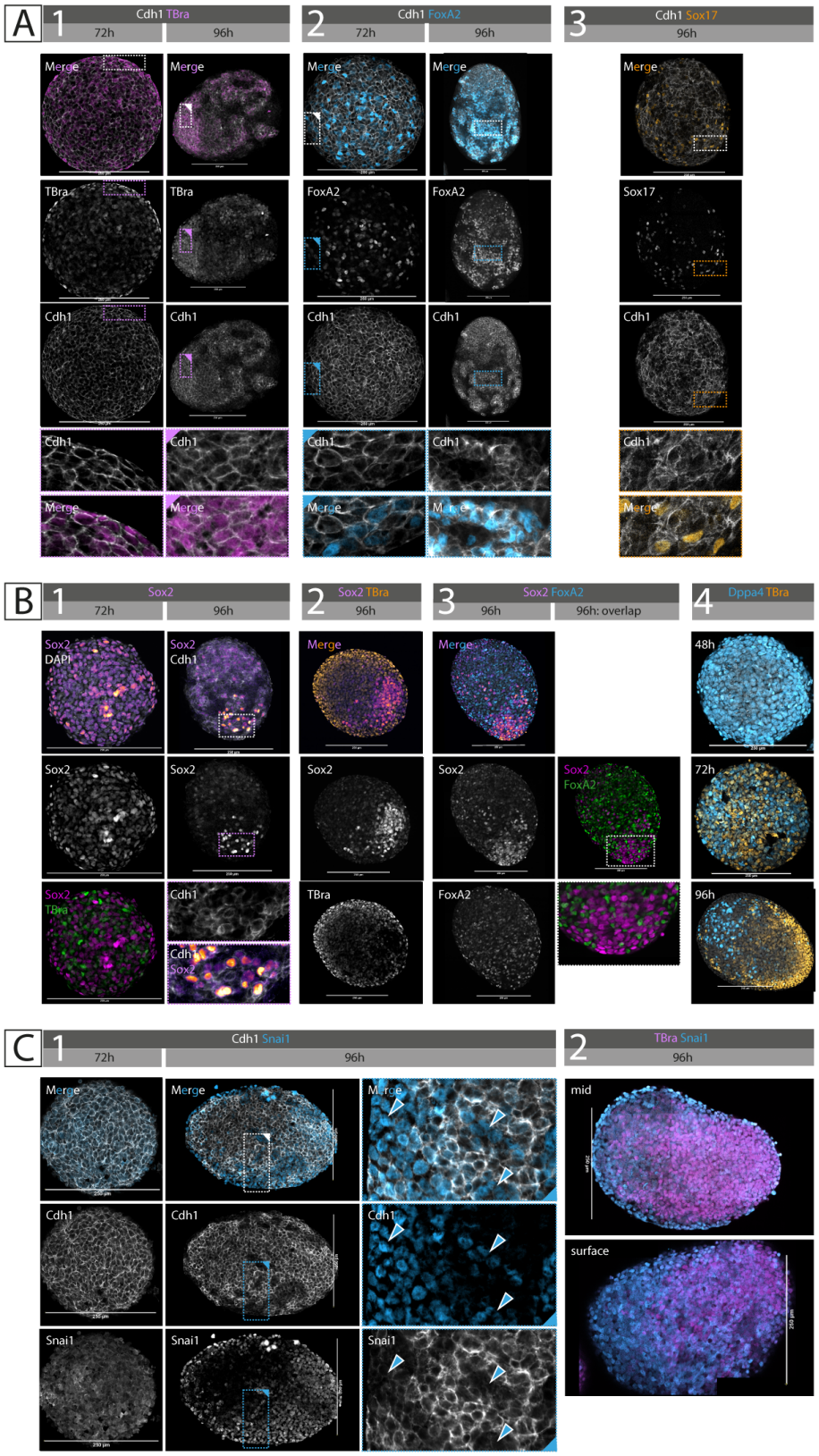

Fig. 3. Endoderm progenitors are epithelial in nature, reside within an epiblast-like compartment, and are spared by classical EMT. (**A**) Immunostaining against the epithelial molecule E-cadherin (Cdh1) at 72h and 96h of Gastruloid development. Notice the drastic fragmentation of epithelial integrity between the two timepoints. Co-stained, are the posterior epiblast and primitive streak marker TBra, and classical endodermal progenitor markers FoxA2 and Sox17. Cells expressing either marker are consistently also CDH1+. (**B**) Immunostaining against the epiblast marker Sox2 shows its segregation at the anterior of the 96h Gastruloid, thus defining a separate domain from FoxA2+ cells. A similar pattern is highlighted by the pluripotency marker Dppa4. (**C**) Immunostaining against the classic EMT regulator Snail-1 (Snai1) shows patterns of expression complementary to those of CDH1. Sna1-mediated EMT is widespread throughout the 96h Gastruloid, and marks cells enveloping the aggregate. Scale bar is always 250um. Marker colocalisation is shown in green and magenta, with double-positive cells appearing white (examples of single-positive and double-positive cells highlighted by single-colour and white arrowheads respectively)

loid, one day later, is radically different: as Gastruloids respond to the CHIR pulse, CDH1 expression becomes patchy. The original CDH1 continuum of the 72h spherical Gastruloid displays signs of clear fragmentation by t=96h (Figure 3A). At the posterior, CDH1+ cells remain clustered and maintain expression of TBra in a configuration analogous to that of the epiblast of the posterior or incipient primitive streak ((Burtscher & Lickert, 2009; Herrmann, 1991), Figure 3A.1), while anteriorly CDH1 continuity is increasingly interrupted by intervening non-epithelial cells (interpreted to be mesoderm). Very interestingly, all FOXA2+ cells seen at this stage are contained within this disaggregating CDH1 core, just as the newly specified SOX17+ cells emerging within such FOXA2+ population (Figure 3A.2 and Figure 3A.3). We never observe FOXA2+ or (FOXA2+/)SOX17+ cells outside of the perimeter defined by the CDH1+ islands.

These findings are particularly significant in that one might naively expect to observe FOXA2+ cells to be leaving their CDH1+ ("epiblast") substrate and for FOXA2+ and FOXA2+/SOX17+ cells to be found in the emerging mesenchymal compartment. Significantly however, FOXA2+ cells leaving the epiblast *in vivo* do not lose CDH1 expression either, but rather relocalise it isotropically until they make contact with and reintegrate the overlaying visceral endoderm (Viotti et al., 2014). The isotropic CDH1 starting point of the Gastruloid at t=72h might thus reconciliate *in vitro* and *in vivo* findings by explaining the retention of SOX17+ cells in the original "epiblast" compartment. More generally, the observation of such pervasive CDH1 expression within Gastruloids, at least those derived from the stem cell line used in this study (see Discussion), challenges the general conception of Gastruloids as mainly mesenchymal organoids, and the mesoderm-heavy focus assigned to their study (van den Brink et al., 2020).

To test the underlying identity of the Cdh1 domain of t=72h and t=96h Gastruloids, and to check whether endodermal identities were indeed emerging and remaining associated with an "epiblast"-like domain, we co-stained Gastruloids for pluripotency and epiblast markers (Figure 3B). Staining for SOX2 shows that the t=72h spheroid is indeed a collection of SOX2+ cells (maintained from earlier timepoints, see data in (Beccari et al., 2018)), and newly emerging TBra+ cells (Figure 3B.1). As such the emerging scattered FOXA2+ population at this stage (also intermingled with TBra+ cells) is likely emerging on this very CDH1+/SOX2+ substrate. Yet, as gastruloid "gastrulation" progresses, the fragmenting epithelial compartment only maintains high SOX2 at a pole (opposite to the TBra pole, i.e. at the anterior, Figure 3B.2), such that the rest of the epithelium, where FOXA2+ and TBra+ identities segregate, shows low or no SOX2 (Figure 3B.3). A similar pattern of segregation and maintenance of potency at the anterior tip of the t=96h gastruloid is highlighted by the observed dynamics of the pluripotency marker DPPA4, marking the entire stem cell aggregate at t=48h, segregating from emerging TBra+ cells at t=72h, and being restricted at the anterior by t=96h (Figure 3B.4).

Our observations are consistent with a model where endodermal identities differentiate without ever leaving the epiblast compartment, or at least where endodermal precursors retain CDH1 expression throughout their development. Indeed, the CDH1+ mass of the t=96h Gastruloid may itself represent different embryonic compartments: one of epiblast, maintaining potency markers at the anterior, and downregulating SOX2 at the posterior where FOXA2+ and TBra+ cells segregate to define respectively distal and proximal posterior epiblast identities, and finally one of FOXA2+/SOX17+ endodermal precursors that would normally be found in the mesenchymal compartment of the embryo but here remain attached to the epiblast given the isotropic CDH1 expression of all other compartments. In either case, we strengthen the case for direct epiblast-to-endoderm transitions that may not require classic EMT or transitions through so-called mesendodermal intermediates (Kubo et al., 2004; Lewis & Tam, 2006; Pfendler et al., 2005; Tada et al., 2005).

Gastruloids undergo widespread EMT, which spares endodermal precursors. To test whether the observed fragmentation of the epithelial core of the Gastruloid is consistent with EMT-like processes one would expect for an *in vitro* model of gastrulation, and how this relates to the apparent failed EMT of endodermal precursors in the Gastruloid, we performed immunostaining for the EMT master regulator Snail (SNAI1) ((Cano et al., 2000; Carver et al., 2001), Figure 3C).

While SNAI1 is only detected at low levels in the cytoplasm of cells of t=72h Gastruloids (all CDH1 positive, as shown before), large swathes of cells with strong nuclear SNAI1 signal are observed at t=96h (Figure 3C.1). Crucially, these patches of SNAI1+ cells are consistently observed to mark the cells intervening between fragments of the CDH1 core. Optical cross-sections at the midplane of t=96h Gastruloids show SNAI1+ cells forming an envelope at the surface, and establishing a posterior to anterior gradient in continuity with the TBra+ posterior (Figure 3C.2).

We thus notice that Gastruloid "EMT" seems to be a generalised rather than localised process, originating at several points within the CDH1+ "epiblast" substrate. Alternatively, SNAI1+ mesodermal types originating from a localised EMT origin may be migrating and physically displacing CDH1+ cells, leading to the observed fragmented appearance. Regardless, the retention of FOXA2+ cells within CDH1+ islands, in an environment of widespread EMT, seems to suggest that these cells are not leaving the epiblast and are either transitioning through endodermal differentiation within their original epiblast-like environment or attempting to leave the epithelium by Snai1-independent mechanisms (Bardot & Hadjantonakis, 2020) and either rapidly reintegrating it at short timescales or remaining attached to it through homotypic CDH1 interactions.

Formation of an endoderm-like primordium.

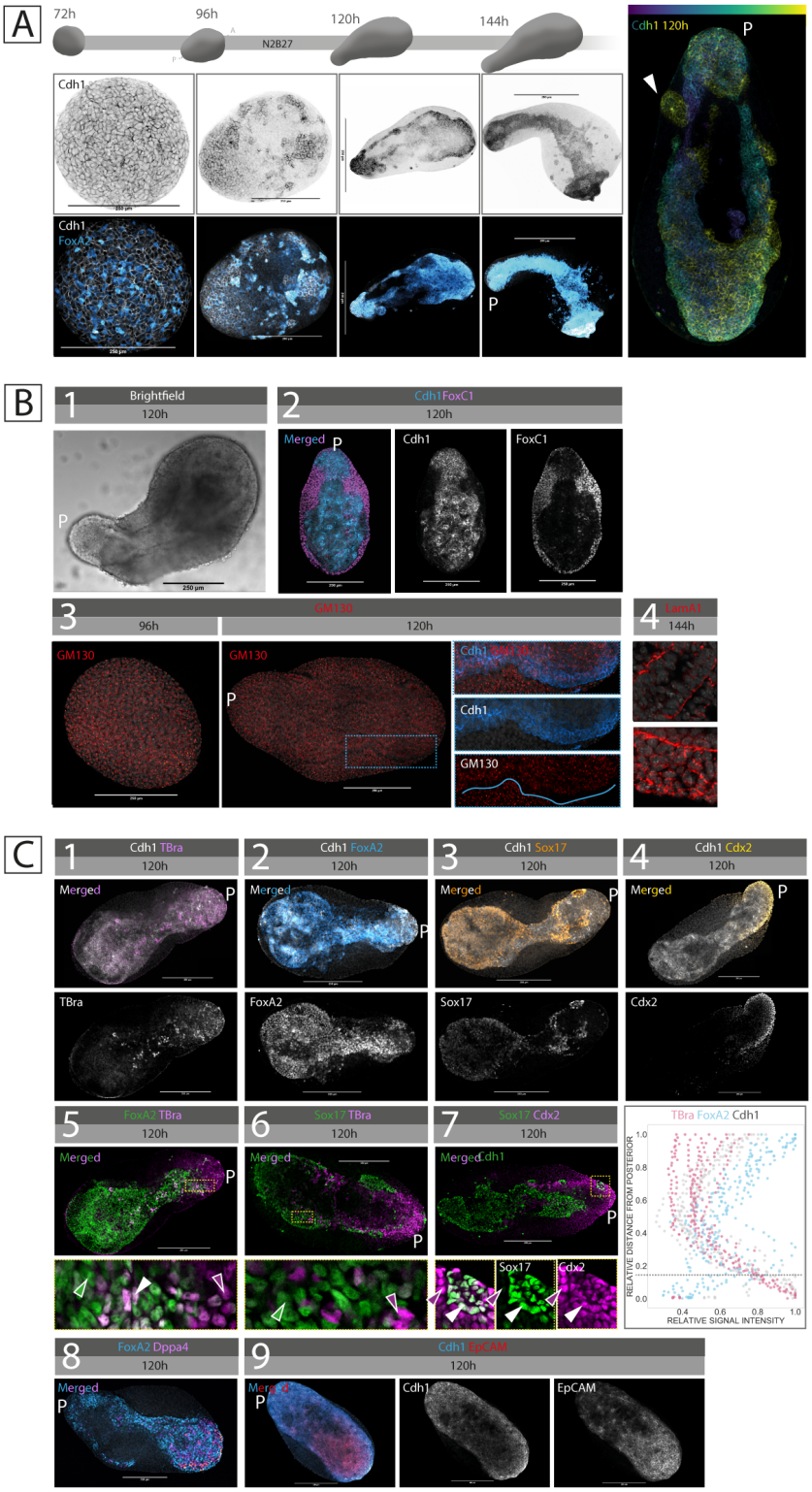

Fig. 4. An epithelial primordium forms at the core of elongating Gastruloids, and shows patterned expression of endodermal markers. (**A**) Representative immunostainings of Gastruloids undergoing elongation and morphogenesis. CDH1+/FOXA2+ cells appear to segregate at the core of the Gastruloid and form an elongated primordium spanning the entire length of the aggregate. On the right, depth-coded projection of the primordium in a 120h Gastruloid. White arrowhead highlights a posterior lateral opening to the surface. (**B**) Macroscopic appearance of the epithelial primordium in its relationship with the overlaying mesodermal wings (FOXC1+). In the second row, maturation of the epithelial identity of the primordium is highlighted by the establishment of apico-basal polarity as hinted by GM130 segregation and basement membrane deposition (Laminin alpha 1 subunit, Lama1). (**C**) Immunostaining of elongated Gastruloids (120h) against the posterior markers TBra and Cdx2, the endodermal markers FoxA2 and Sox17, the pluripotency marker DPPA4, and the epithelial marker EpCAM to see their localisation within the CDH1+ primordium. A summary expression profile of some of these markers is also provided (gray dotted line indicating the separation between the domain of high TBra but low FoxA2, and that of high FoxA2 and low TBra).Scale bar is always 250um. Marker colocalisation is shown in green and magenta, with double-positive cells appearing white (examples of single-positive and double-positive cells highlighted by single-colour and white arrowheads respectively). P = posterior of the Gastruloid.

The epithelial core of the Gastruloids undergoes dramatic architectural rearrangements. To evaluate the later fate of endodermal cells within the gastruloid core, we further tracked Cdh1, FoxA2, and Sox17 patterns of expression as the Gastruloid undergoes morphogenesis and elongation from t=96h onward ((Beccari et al., 2018), Figure 4).

Strikingly, the fragmented CDH1+ core of the t=96h Gastruloid gradually re-organises in complex and streamlined elongated architectures extending along the entire length of the Gastruloid (Figure 4A). Over time, the tear-drop shaped, fragmented CDH1+ core of the t=96h Gastruloid tapers into a multi-branched, whisk-shaped epithelial primordium (t=120h, 144h), which in turn resolves in a single rod-like tissue that follows the outer geometry of the Gastruloid (144h onward). This epithelial structure emerges on the surface of the Gastruloid at the very posterior (and is indeed an extension of it), sometimes displaying multiple surface points in the region (white arrowhead Figure 4A, right), and occasionally also resurfaces at the anterior at much later timepoints (t=168h). Crucially, cells of this epithelial core are marked by FoxA2 at all stages of development (Figure 4A, bottom row). Macroscopically, this epithelial mass is already distinguishable in brightfield as a rod-like structure of compact cells extending from the posterior and gradually becoming enveloped by anteriorly-extending wings of loser, mesenchymal-like cells (Figure 4B.1). Co-staining of CDH1 with the pan-mesodermal marker FoxC1 (Sasaki & Hogan, 1993) clearly identifies the enveloping tissue as mesodermal (whose differentiation will give rise to the variety of trunk and cardiac structures described in (Rossi et al., 2019; van den Brink et al., 2020; Veenvliet et al., 2020)) and highlights a previously under-appreciated architectural organisation of the Gastruloid model, with interfacing epithelial and mesenchymal tissue (Figure 4B.2). Interestingly, such coupled configuration raises the possibility that the two compartments may engage in productive developmental interaction, possibly stimulating the development of cells types that would not otherwise emerge in either alone (as described *in vivo* e.g. in (Han et al., 2019)).

Interestingly, the CDH1+ primordium appears to undergo epithelial maturation over time. Whereas CDH1+ cells of the t=72h Gastruloid represented more an epithelioid state, with expression of epithelial markers but without epithelial architecture, the t=120h and onward CDH1 mass shows signs of apico-basal polarity with polarised arrangement of GM130 (Figure 4B.3), and gradual deposition of discontinuous stretches of laminin (LAMA1 subunit) at the interface with the overlaying mesoderm (Figure 4B.4). We could not prove the existence of a continuous lumen within this epithelium, suggesting this structure to be more akin to a plastic epithelial mass rather than a defined continuous tube (data not shown). When present, supernumerary points of contact with the posterior surface of the Gastruloid do however seem to be consistently associated with rosetting and local invagination (see Figure 4A), even though we cannot at this point demonstrate continuity of these cavities with the rest of the CDH1 core.

Endodermal patterning along the AP axis of the Gastruloid. Having observed such dramatic and unexpected epithelial rearrangements over late Gastruloid development, and such tight association between this newly formed CDH1 core and the endodermal marker FOXA2, we proceeded to further characterise the identity of these cells and their possible patterning along the AP axis (Figure 4C, indeed observed for cells of the overlaying mesodermal compartment (Beccari et al., 2018; van den Brink et al., 2020)).

Matching the surprising increase in the number of CDH1+/FOXA2+ cells from t=96h to t=120h, where FOXA2 seems to mark almost the entirety of the CDH1+ primordium, SOX17 immunostaining also reveals a surprising increase in SOX17+ numbers, with cells extending from the neck of the CDH1 primordium (and often from the "hole" like surface openings described above) up to anteriormost extremity of the epithelium (Figure 4C.2 and Figure 4C.3). Immunostaining for the posterior primitive streak and tailbud marker TBra (Figure 4C.1) reveals that while FOXA2+ and SOX17+ cells may well be in continuity with the CDH1+/TBRA+ Gastruloid tip, they organise themselves just anterior to it. Batch quantification of signal intensity along the AP axis of Gastruloids (see plot in Figure 4C) indeed highlights reproducible patterning where the posterior 5th of the CDH1 primordium is marked by TBra+/CDH1+/FOXA2- cells, while the rest is populated by TBra-/CDH1+/FOXA2+ (and SOX17+) cells, an epithelialised endoderm whose continuity with the TBra+ pole might be explained by persistent homotypic interaction between different CDH1+ tissues. Of note, few TBra+ cells do seem to also extend deeper into the FOXA2+ domain (Figure 4C.5), and constitute a CDH1+/TBra+/FOXA2+ population that may be consistent with midline embryonic structures (Burtscher & Lickert, 2009; Yamanaka et al., 2007).

At the very posterior of the Gastruloid (and thus of the CDH1 primordium), the posterior marker CDX2 (Beck et al., 1995) marks not only the TBra+/CDH1+ cells of the gastruloid tip, and CDH1- mesenchymal cells emerging laterally from it (Figure 4C.4), but also (CDH1+/)SOX17+ cells at the posterior limit of the SOX17+ domain (Figure 4C.7). Comparison of these structures with the caudal intestinal portal forming during *in vivo* endoderm development (Beccari et al., 2018) are enticing but will need to wait further characterisation. At the opposite end (anterior), DPPA4+ cells intermingle with FOXA2+ endoderm (Figure 4C.8), likely representing a surprising maintenance of pluripotency from the earliest timepoints of Gastruloid differentiation (giving their continuity with DPPA4+ cells at all previous timepoints). On this regard, other groups have interestingly reported the presence of Primordial-Germ-Cell-like cells, marked by DPPA3+, in association with the endodermal component (Veenvliet et al., 2020).

Finally, we identify the cell surface protein EpCAM as another marker of the entire primordium, with expression almost completely overlapping that of CDH1 (Figure 4C.9), yet with an apparent enrichment towards the anterior. The expression of EpCAM distinguishes the (CDH1+/)SOX17+ cells we observe as being indeed endodermal, given that this same marker also characterises endothelial progenitors (which would however be EpCAM-) at around the same developmental timepoints (Choi et al., 2012). Interestingly, EpCAM staining appears enriched in the region of the CDH1 primordium occupied by SOX17+ cells, hinting that combinations of cell-surface markers might drive further sub-sorting of different epithelial combinations within this same CDH1+ core. Here, the posterior of the primordium would represent a "posterior epiblast"-like, CDH1+/EpCAMlow/TBra+ domain; and the anterior a CDH1+/EpCAMhigh/FOXA2+/Sox17+ "endoderm"-like domain. Further characterisation will highlight whether more refined endoderm identities pattern such domain (Nowotschin et al., 2019b), and whether the absent contribution of extraembryonic cells biases such identities to specific domains.

Discussion

Cells expressing endodermal markers, and gene expression patterns consistent with endodermal identities, have been described in several previous Gastruloid studies (Beccari et al., 2018; Pour et al., 2019; Turner et al., 2017; van den Brink et al., 2020, 2014; Veenvliet et al., 2020). Given the often mesoderm- and neurectoderm-focused perspective of most of these publications however, these descriptions have often not taken centre stage, or even been expanded on beyond surface level descriptions (with the exception of (Pour et al., 2019), see later). Of notice is the fact that FoxA2 and Sox17, indeed classical endoderm markers, are also expressed in other embryonic cell types at the same developmental stages where the endoderm and the gut tube are specified. As such, while detecting either of these markers in the embryo may exclude non-endodermal identities given the spatial and temporal context of the observation, the same cannot be said in Gastruloids, where the full extent of the cell types generated is still under characterisation (van den Brink et al., 2020), and where temporal alignment with *in vivo* developmental stages is equally uncertain (Beccari et al., 2018). Accordingly, FOXA2 marks the endoderm just as much as the neural floorplate and the notochord; TBra marks posterior hindgut as well as posterior epiblast, notochord, and neuromesodermal progenitors; and SOX17 marks both endoderm and endothelial progenitors (Choi et al., 2012).

Regardless, original descriptions of Gastruloids were indeed already describing polarised emergence of cells expressing both FOXA2 and SOX17, taken as to indicate endodermal identity (van den Brink et al., 2014). A compact FOXA2+ domain was thus seen to cluster at the posterior of late stage Gastruloids, with SOX17+/TBra- cells occupying this very FOXA2+ domain and internalising within epithelial vesicles. We presently cannot reconcile this posteriormost pattern of expression with what we describe here, but we do notice that in those cell lines where the CDH1 primordium does not extend throughout the length of the aggregate it segregates as a compact mass at the posterior (data not shown). The described invagination of SOX17+ cells may however indeed explain the surface continuity of the posterior CDH1 primordium that we see in the neck region of some of our Gastruloids.

More complete Sox17 patterns have been described in (Turner et al., 2017), where the use of a reporter highlights the formation of *Sox17*+ midline, tubular-shaped patterns in elongating gastruloids. The study likens these cells to ventral endodermal cells of the E8.5 mouse embryo but however does not investigate the matter further. Based on our result, and the extensive SOX17 positivity of the CDH1 primordium we describe here, we would expect the reporter line used in (Turner et al., 2017) to equally give rise to an internal endodermal primordium. Interestingly, the early *Sox17* dynamics described in the paper also seem to confirm what we here infer by immunostaining: Sox17+ cells emerging towards the anterior pole of the early Gastruloid and then expanding to occupy a relatively more posterior domain.

SOX17+ cells were also identified in (Beccari et al., 2018), and described as forming tubular structures based on DAPI counterstaining. More importantly, the publication describes gene expression dynamics associated with advanced endoderm maturation: the early upregulation of markers such as Gsc and Cdx2, upregulation of Cer1 during elongation, and expression of posterior foregut markers during later development (Nedn, Sorcs2, Pax9, Pyy, Shh, Krt18). *In situ* hybridisation patterns for some of these markers are again consistent with the presence of an internal endodermal structure. Still, detailed spatial characterisation is lacking, and the Gastruloid remains framed as a mainly mesenchymal neuromesodermal aggregate. Further validation of the maturation of endodermal identities (but crucially again not of their actual spatial organisation) can also be found in the single-cell transcriptomics data generated by (van den Brink et al., 2020), which detect a cluster of cells postulated to represent definitive endoderm as expressing markers Epcam, Col4a1, Sox17.

Most recently, tubular structures populated by FOXA2+ and some SOX17+ and TBra+ cells have also been described in (Veenvliet et al., 2020) even though our results would seem to suggest that embedding of the Gastruloid in extracellular matrix components is not necessary to observe endoderm morphogenesis, and that this tissue may actually already organise its own extracellular matrix environment. Unlike mesoderm thus, which seems to require ECM cues for productive mesenchymal to epithelial transition (van den Brink et al., 2020; Veenvliet et al., 2020), morphogenesis of the endoderm appears to be intrinsic to the tissue.

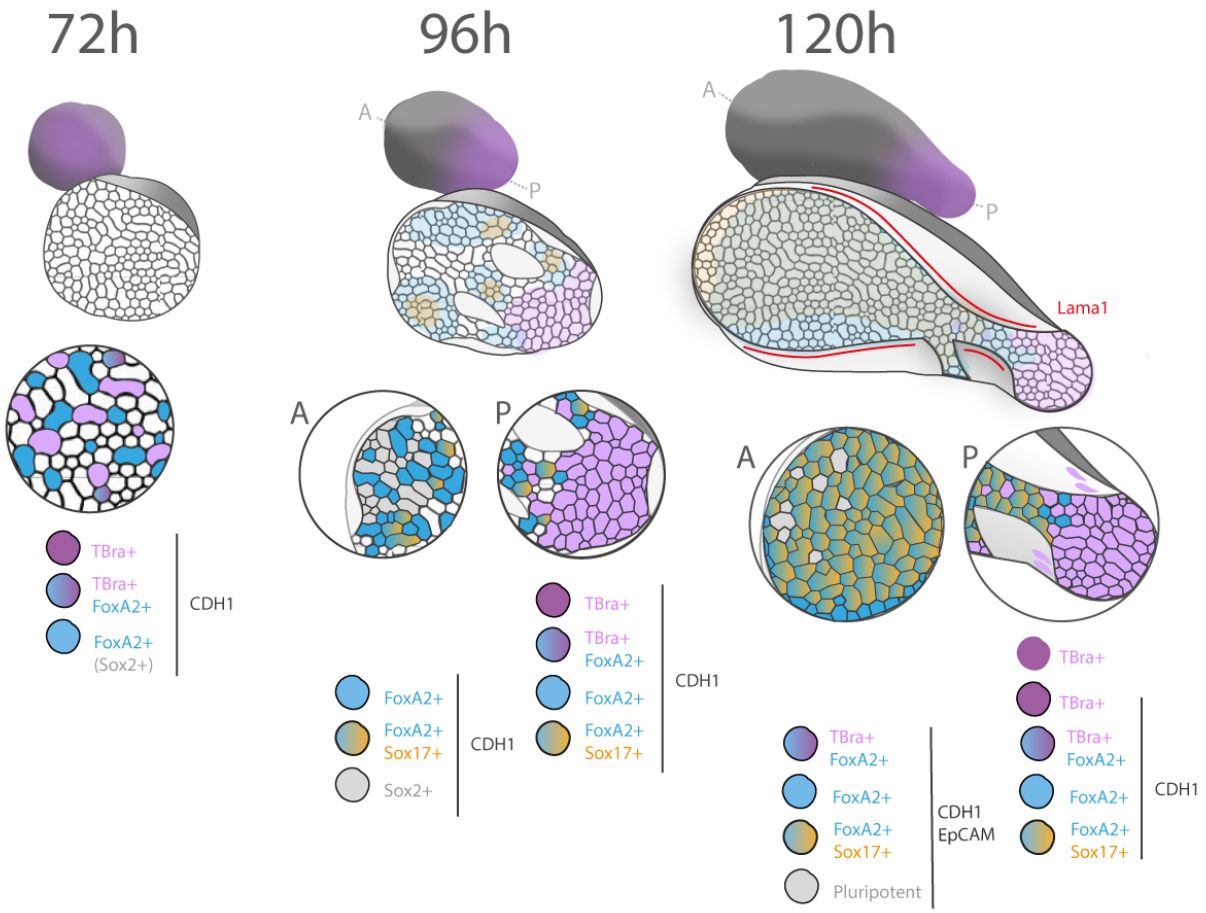

Fig. 5. Endoderm specification and patterning in Gastruloids, a summary. At 72h of development, Gastruloids appear to be an epithelioid spheroid with intermingled TBra+ and FOXA2+ CDH1+ cells. We interpret FOXA2+ cells to also be SOX2+, and this spheroid to represent the posterior epiblast of the early gastrulating mouse embryo, with equally intermingled populations. Between 72h and 96h, Gastruloids undergo widespread Snai1-dependent EMT: mesenchymal types emerge and CDH1 continuity fragments. At the posterior, CDH1+/TBra+ cells define a proximal posterior epiblast compartment and FOXA2+ cells define a distal posterior epiblast region. Anteriorly, the CDH1 domain remains SOX2+. Within the CDH1+/FOXA2+ domains, SOX17+ cells emerge. In the embryo these cells would be expected to be found in the mesenchymal compartment. At t=120h, the CDH1+ primordium organises as a maturing epithelium extending along the entire length of the aggregate, enveloped by mesenchymal (mesoderm) cells. FOXA2+ and SOX17+ cells pattern along this primordium, just anteriorly to a posterior-epiblast-like TBra+/CDH1+ domain. EpCAM also seems to mark this very CDH1 primordium, with an anterior enrichment.

Perhaps the most attentive detailing of endoderm emergence in Gastruloids has been performed by (Pour et al., 2019), who elegantly used a TBra/Sox17 double reporter cell line to document expression of these two markers in a temporal sequence consistent with what we describe in this study. *Sox17*+ cells emerge around 1 day after CHIR exposure, intermingled within a field of TBra+ cells. While the authors also see strong association between *Sox17* expression and epitheliality (CDH1 positivity), they do seem to identify a stage where such Sox17+ cells are CDH1-, and indeed favour an interpretation that supports a mesendodermal origin of endodermal precursors. In our observations, Gastruloids start in a epithelioid configuration where cells have mesenchymal character but express CDH1, and in which TBra+, FOXA2+, and SOX17+ cells thus all emerge in a CDH1+ context.

The observations we report here bring centre stage the question of the epithelial character of endodermal precursors, and its link to the fate (both in terms of identity and of location) of these cells. We expand on previous Gastruloid studies by taking into consideration multiple markers of endodermal identity and documenting their dynamics in relation to one another, and notably by also tracking these cells over time as they undergo morphogenesis. We further also describe sorting of these cells into a complex primordium with maturing epithelial architecture and coarsely patterned domains of gene expression along the AP axis of the organoid. We currently prefer refraining from likening this primordium to the early gut tube of the embryo, as more detailed characterisation is underway. At this point, our observations are consistent with a model whereby SOX17+ cells never leave their epithelial environment (initially, the "epiblast"-like domain) and do not need to transition through a mesenchymal state, at least not through classic Snai1-mediated EMT. We speculate that, if SOX17+ endodermal cells are not being directly specified within the FOXA2+ epiblast, the SOX17+ cells that we incongruously see in this compartment are a result of these cells sticking to neighbours

with the same epithelioid character. While in the embryo the isotropic relocalisation of CDH1 associated with egressed endodermal cells might be compatible with segregation from both epiblast (columnar epithelium) and visceral endoderm (squamous epithelium), and indeed reintegration of Sox17+ cells requires re-polarisation, the situation is different in Gastruloids. In our system, FOXA2+ and SOX17+ cells are emerging not in a polarised columnar epithelium, but in a context that already displays isotropic CDH1 localisation, such that these cells may remain stuck in their original compartment just by virtue of homotypic interactions. Interestingly, and during preparation of this manuscript, the use of a Cdh1 live reporter by (Hashmi et al., 2020) has shown fragmentation and early sorting dynamics consistent with what we show here by immunostaining, and the authors explain these sorting dynamics by differences in interfacial tension across cell types. Later in development we here further observe an expansion of the endodermal population and its internalisation within the core of the Gastruloid as the surface of the aggregate start being populated by an increasing number of mesodermal cells. Interestingly, the relative position of different epithelial populations may here again be explained by the expression of different combinations of cell-surface adhesion molecules, a common sorting mechanisms (Toda et al., 2018) that sees here some support from the biased EpCAM distribution within our CDH1 primordium, enriched in the domains occupied by endodermal cells.

Our identification of a maturing epithelial structure throughout late Gastruloid development, contrasting with the overlaying mesenchymal mesodermal tissues enveloping it, reframes expectations regarding the extent to which fate and morphogenesis can spontaneously arise *in vitro*. While gastruloids have traditionally been pictured as aggregates of fates without corresponding organisation (van den Brink et al., 2020), we start to see increasing examples where such missing morphogenesis does occur. As already shown by (Bérenger-Currias et al., 2020; Veenvliet et al., 2020) this can be transformatively brought about by the addition of diluted ECM components or extraembryonic cell types. We here show that differences in epithelial identities between emerging cell types may already be sufficient to generate simple architectures, and that complex epithelia may spontaneously organise *de novo* in Gastruloids. Still, the extent to which the elaborate morphogenesis seen here is cell-line specific remains to be defined. Current literature contains examples of Gastruloids from a variety of cell lines and mouse backgrounds that do indeed originate such internal epithelial primordia (Beccari et al., 2018; Rossi et al., 2019) (or where we infer such primordium to be what described (Turner et al., 2017; Veenvliet et al., 2020)), as well as of Gastruloids where such structures do not seem to appear (van den Brink et al., 2020, 2014) and where CDH1 tissue segregates to the posteriormost tip of the aggregates instead. We favour the hypothesis that these differences likely correlate to intrinsic cell-line biases in core signalling pathways, and/or on the very degree of epitheliality maintained by these cells by the time they are exposed to CHIR. A systematic assessment of the cell-line specific differences in these key parameters remains to be performed. Regardless, the stratified nature of endodermal and mesodermal tissues we here observe is at least broadly comparable to the configuration of endoderm and mesoderm in the embryo, and it is interesting to speculate that this interfacing may favour the development of more advanced cell fates by reciprocal signalling interactions, as *in vivo* (Bardot & Hadjantonakis, 2020; Han et al., 2019).

We will keep this document up to date and share any further characterisation of the CDH1+ endodermal primordium, and whether FOXA2+ and SOX17+ cells that populate it at 120h further pattern according to the anterior-posterior cues of the aggregate, and to which endodermal organ identities they might give rise to. As per the classical paradigm offered by *in vitro* developmental models (Shahbazi & Zernicka-Goetz, 2018), we trust that the extent to which this will match *in vivo* gut tube development will highlight important developmental principles in both systems.

Materials and methods

Cell culture. mESCs ("SBR" Sox1/TBra double reporter cell line described in (Deluz et al., 2016); CRG8 cells of 129P2 background (RRID:CVCL_3987, (Mountford et al., 1994))) were cultured in tissue-culture-treated, non-gelatinised, 6well plates, in 10%Serum Medium with added 2i and LIF. Cells were split every third day, by washing in PBS-/-, adding Accutase for ~3min RT, and collecting the resulting cell suspension in a clean centrifuge tube. The Accutase of the cell suspension was then diluted out 1:10 in 10% Serum Medium, and cells were pelleted by centrifuging 200xg, 4min, 4°C. After aspirating out the supernatant, the pellet was resuspended in 1mL 10% Serum Medium to a single cell suspension, and cell density was counted with a haemocytometer. Around 65000-75000 cells were transferred to a new well with 2mL pre-equilibrated 10%Serum Medium (6750-7800 cells/cm2). Cells were then left in a humidified incubator, 37°C, 5% CO_2, until use or until further splitting 3 days later. NOTE: In most cases, splitting was coupled to Gastruloid generation. In those cases, the cell pellet was resuspended in N2B27 rather than 10% Serum Medium + 2i and LIF. A complete, step-by-step, protocol is available at:https://dx.doi.org/10.17504/protocols.io.7xbhpin
Recipes:
10% Serum Medium: 86.8% DMEM, high glucose, with GlutaMAX (L-Alanyl-Glutamine, final concentration: 3.45mM), 10% ES-grade Foetal Bovine Serum, 100U/mL Penicillin, 100ug/mL Streptomycin, 0.1mM Non Essential Amino Acids, 1mM Sodium Pyruvate, 0.1mM beta-mercaptoethanol
10% Serum Medium + 2i and LIF: add 3uM CHIR99021, 1uM PD0325901,and 100u/mL LIF.

Gastruloid generation. mESCs were washed in PBS-/-, detached from adherent culture with Accutase (~3min, RT), and collected in a centrifuge tube. The Accutase in the

cell suspension was then diluted out 1:10 in 10% Serum Medium, and cells were pelleted by centrifuging 200xg, 4min, 4C. The supernatant was removed, and the pellet was washed by resuspension in 10mL PBS-/-. Cells were re-pelleted by centrifuging 200xg, 4min, 4C and washed once more in 10mL fresh PBS-/-. After re-pelleting once more (200xg, 4min, 4C), the pellet was dissociated as a single-cell suspension in 1mL N2B27 Medium. Cells were counted with a haemocytometer, and, for each plate of Gastruloids made, 37500 cells were transferred to 5mL fresh N2B27 (7.5 cells/uL final concentration). The cell suspension was distributed as 40uL droplets (=300 cells/droplet) in wells of a U-bottomed, low-adhesion, 96 well plate, and the plates were left for 120h in a humidified incubator, 5% CO_2, 37°C. At 48h after plating, 150uL of 3uM CHIR99021 N2B27 were added to each well, and this solution was substituted with fresh N2B27 (no CHIR) every 24h after that. A step-by-step detailed protocol is available at: https://dx.doi.org/10.17504/protocols.io.9j5h4q6 Recipes: 10% Serum Medium: 86.8% DMEM, high glucose, with 3.97mM GlutaMAX (L-Alanyl-Glutamine, final concentration: 3.45mM), 10% ES-grade FBS, 100U/mL Penicillin , 100ug/mL Streptomycin, 0.1mM Non Essential Amino Acids, 1mM Sodium Pyruvate, 1mM beta-mercaptoethanol. N2B27: 47.4% Neurobasal Medium, 47.4% DMEM/F-12, with 2.50mM GlutaMAX (L-Alanyl-Glutamine, final concentration: 1.18mM), 1mM GlutaMAX Supplement (total concentration: 2.18mM), 100U/mL Penicillin , 100ug/mL Streptomycin, 0.1mM Non Essential Amino Acids, 1mM Sodium Pyruvate, 1mM beta-mercaptoethanol, 1% B27Supplement, serum-free, 0.5% N-2 Supplement.

Gastruloid immunostaining. Gastruloids were collected at every given timepoint, washed in PBS-/-, and fixed in 4% PFA in PBS-/-, for 2h, 4C, on a low-speed orbital shaker; or 45min, RT, static. Gastruloids were then washed in PBS+FT (PBS-/-, 10% ES-grade Foetal Bovine Serum, 0.2% Triton-X100), and blocked and permeabilised in PBS+FT for 1h, RT, static. Primary antibody solutions were then prepared in PBS+FT, with 2ug/mL DAPI. Samples were stained overnight, 4C, on a low-speed orbital shaker. Similarly, secondary antibody solutions were prepared in PBS+FT, 2ug/mL DAPI, and samples were stained overnight, 4C, on a low-speed orbital shaker. Gastruloids were mounted in Fluoromount-G mounting medium (no spacers), and slides kept at 4C long term. All antibody solutions were washed away after incubation by washes in PBS+FT. A detailed, step-by-step protocol is available at: https://dx.doi.org/10.17504/protocols.io.7tzhnp6. Secondary antibodies used were all from Thermo Fisher Scientific: donkey anti-mouse IgG Alexa 647 (CAT#A-31571, RRID:AB_162542); donkey anti-rabbit IgG Alexa 488 (CAT#A-21206, RRID:AB_2535792), Alexa 568 (CAT# A-10042, RRID:AB_2534017), or Alexa 647 (CAT# A-31573, RRID:AB_2536183); donkey anti-rat IgG Alexa 488 (CAT#A-21208, RRID:AB_2535794), goat anti-rat Alexa 568 (CAT#A-11077, RRID:AB_2534121), or Alexa 647 (CAT#A-21247, RRID:AB_141778); donkey anti-goat IgG Alexa 488 (CAT#A-11055, RRID:AB_2534102), or Alexa 568 (CAT#RRID:AB_2534104). Details about the primary antibodies used are provided as a supplementary .csv file.

Gastruloid imaging and image processing. Brightfield images of Gastruloids were taken on either a Nikon Ti inverted spinning-disk microscope (for the series in Figure 2A), or an Olympus CellR inverted widefield microscope (for the image on Figure 4B, UPLAN S APO 10x/0.40 air objective, CCD Grayscale Hamamatsu ORCA ER B7W Camera; Olympus XCellence software for data capture). Both microscope setups had CO2 and temperature control (37°C and 5% CO_2). Immunostained Gastruloids were imaged on a Zeiss LSM700 inverted confocal microscope (Plan-Apochromat 20x/0.80 air objective, motorized stage, LED Lumencor SOLA Illumination, CCD Grayscale Axiocam MRm (B/W) Camera; ZEN 2009 software for data capture) or on a Zeiss LSM780 inverted confocal microscope (for the CDH1 projection in Figure 4A, Plan-Apochromat 20x/0.80 air objective, motorized stage). Images were opened, stitched, and processed for publication (LUT assignment, channel display, min and max intensity thresholding based on no-primary control) using the Fiji ImageJ distribution (Rueden et al., 2017; Schindelin et al., 2012), and the "Grid/Collection Stitching" plugin therein (Preibisch et al., 2009). The depth-coded reconstruction in Figure 4A was generated using the "Temporal-Color Code" (https://imagej.net/Temporal-Color_Code) function. The blue, orange, and purple LUTs used throughout the figures were designed by Christophe Laterrier (https://github.com/cleterrier/ChrisLUTs, "BOP" palette).

Quantification of AP patterning. Batch quantification of immunostaining signal intensity along the AP axis of the Gastruloids was performed through a custom processing pipeline available as a Jupyter notebook at https://doi.org/10.5281/zenodo.3884238 and outlined as follows (step-by-step walk through provided in the notebook itself). The pipeline takes two inputs: i) the multichannel raw image resulting from the scan of an entire microscope slide of immunostained and mounted Gastruloids (here acquired on a GE Healthcare IN Cell Analyzer 2200 automated microscope) and ii) hand-traced line coordinates defining the central axis of each Gastruloid on the slide (starting from the posterior). At early timepoints where the posterior of the Gastruloid is not distinguishable morphologically, the area of TBra polarisation is to be used instead. The script then subdivides each interval of the line ROI provided into n finer intervals of equal length (thus avoiding to have to manually draw a line with high number of points; here n=10), and for each point along the line it defines a non-overlapping polygon mask covering an area of thickness N (here N=500px) across the line and whose lateral edges are orthogonal to the line itself at each side of the point. Having computed the mask, the

script then assigns the total signal intensity recovered in the area to the point of the line ROI around which the polygon was constructed, thus effectively assigning signal intensities to points that can be ordered along an x-axis. These raw values are then normalised by the number of cells in the area (using the DAPI nuclear intensity as a proxy) and both position along the length of the Gastruloid and signal intensity are normalised to the absolute length of the Gastruloid and to the maximal DAPI-normalised intensity value. The script outputs lineplots and scatterplots for each Gastruloid analysed, summary lineplots and scatterplots with collated data of all gastruloids analysed, and the tabulated raw data for re-use.

ACKNOWLEDGEMENTS

We would like to acknowledge the work and support provided by the staff of many of the EPFL core facilities: notably, the staff of the BioImaging and Optics Platform (BIOP), the staff of the Biomolecular Screening Facility (BSF), and the staff of the Histology Core Facility. We also want to acknowledge the work of the entire staff of the Glassware Washing facility (Laverie), as well as all of EPFL cleaning staff. This work would have not been possible without their contribution. The pipeline designed to quantify AP patterning in Gastruloids was constructed in collaboration with Paul Gerald Layague Sanchez and Arianne Bercowsky-Rama, whom we sincerely thank. We would also like to acknowledge our lab manager Stephanie Boy-Rottinger for her heartfelt support throughout. In addition, we are thankful to Ricardo Henriques for kindly sharing the template that was used to format this preprint. This research was funded by a Sinergia grant (CRSII5_189956) from the Swiss National Science Foundation and Ecole Polytechnique Fédérale de Lausanne (EPFL).

COMPETING FINANCIAL INTERESTS

The authors declare no competing financial interests.

Bibliography

Allman, G. J. (1854). On the anatomy and physiology of Cordylophora a contribution to our knowledge of the tubularian zoophytes. *Abstracts of the Papers Communicated to the Royal Society of London*, *6*, 319–321.
URL https://doi.org/10.1098%2Frspl.1850.0118

Arnold, S. J., & Robertson, E. J. (2009). Making a commitment: cell lineage allocation and axis patterning in the early mouse embryo. *Nature Reviews Molecular Cell Biology*, *10*(2), 91–103.
URL https://doi.org/10.1038%2Fnrm2618

Baillie-Johnson, P., van den Brink, S. C., Balayo, T., Turner, D. A., & Arias, A. M. (2015). Generation of Aggregates of Mouse Embryonic Stem Cells that Show Symmetry Breaking Polarization and Emergent Collective Behaviour emIn Vitro/em. *Journal of Visualized Experiments*, (105).
URL https://doi.org/10.3791%2F53252

Bardot, E., Calderon, D., Santoriello, F., Han, S., Cheung, K., Jadhav, B., Burtscher, I., Artap, S., Jain, R., Epstein, J., Lickert, H., Gouon-Evans, V., Sharp, A. J., & Dubois, N. C. (2017). Foxa2 identifies a cardiac progenitor population with ventricular differentiation potential. *Nature Communications*, *8*(1).
URL https://doi.org/10.1038%2Fncomms14428

Bardot, E. S., & Hadjantonakis, A.-K. (2020). Mouse gastrulation: Coordination of tissue patterning specification and diversification of cell fate. *Mechanisms of Development*, (p. 103617).
URL https://doi.org/10.1016%2Fj.mod.2020.103617

Beccari, L., Moris, N., Girgin, M., Turner, D. A., Baillie-Johnson, P., Cossy, A.-C., Lutolf, M. P., Duboule, D., & Arias, A. M. (2018). Multi-axial self-organization properties of mouse embryonic stem cells into gastruloids. *Nature*, *562*(7726), 272–276.
URL https://doi.org/10.1038%2Fs41586-018-0578-0

Beck, F., Erler, T., Russell, A., & James, R. (1995). Expression of Cdx-2 in the mouse embryo and placenta: Possible role in patterning of the extra-embryonic membranes. *Developmental Dynamics*, *204*(3), 219–227.
URL https://doi.org/10.1002%2Faja.1002040302

Bérenger-Currias, N. M. L. P., Mircea, M., Adegeest, E., van den Berg, P. R., Feliksik, M., Hochane, M., Idema, T., Tans, S. J., & Semrau, S. (2020). Early neurulation recapitulated in assemblies of embryonic and extraembryonic cells.
URL https://doi.org/10.1101%2F2020.02.13.947655

Burtscher, I., & Lickert, H. (2009). Foxa2 regulates polarity and epithelialization in the endoderm germ layer of the mouse embryo. *Development*, *136*(6), 1029–1038.
URL https://doi.org/10.1242%2Fdev.028415

Cano, A., Pérez-Moreno, M. A., Rodrigo, I., Locascio, A., Blanco, M. J., del Barrio, M. G., Portillo, F., & Nieto, M. A. (2000). The transcription factor Snail controls epithelial–mesenchymal transitions by repressing E-cadherin expression. *Nature Cell Biology*, *2*(2), 76–83.
URL https://doi.org/10.1038%2F35000025

Carlson, B. M. (2014). Digestive and Respiratory Systems and Body Cavities. In *Human Embryology and Developmental Biology*, (pp. 335–375). Elsevier.
URL https://doi.org/10.1016%2Fb978-1-4557-2794-0.00015-2

Carver, E. A., Jiang, R., Lan, Y., Oram, K. F., & Gridley, T. (2001). The Mouse Snail Gene Encodes a Key Regulator of the Epithelial-Mesenchymal Transition. *Molecular and Cellular Biology*, *21*(23), 8184–8188.
URL https://doi.org/10.1128%2Fmcb.21.23.8184-8188.2001

Chazaud, C., Yamanaka, Y., Pawson, T., & Rossant, J. (2006). Early Lineage Segregation between Epiblast and Primitive Endoderm in Mouse Blastocysts through the Grb2-MAPK Pathway. *Developmental Cell*, *10*(5), 615–624.
URL https://doi.org/10.1016%2Fj.devcel.2006.02.020

Choi, E., Kraus, M. R.-C., Lemaire, L. A., Yoshimoto, M., Vemula, S., Potter, L. A., Manduchi, E., Stoeckert, C. J., Grapin-Botton, A., & Magnuson, M. A. (2012). Dual Lineage-Specific Expression of Sox17 During Mouse Embryogenesis. *STEM CELLS*, *30*(10), 2297–2308.
URL https://doi.org/10.1002%2Fstem.1192

Davies, J. (2017). Using synthetic biology to explore principles of development. *Development*, *144*(7), 1146–1158.
URL https://doi.org/10.1242%2Fdev.144196

Deluz, C., Friman, E. T., Strebinger, D., Benke, A., Raccaud, M., Callegari, A., Leleu, M., Manley, S., & Suter, D. M. (2016). A role for mitotic bookmarking of SOX2 in pluripotency and differentiation. *Genes & Development*, *30*(22), 2538–2550.
URL https://doi.org/10.1101%2Fgad.289256.116

Dufort, D., Schwartz, L., Harpal, K., & Rossant, J. (1998). The transcription factor HNF3beta is required in visceral endoderm for normal primitive streak morphogenesis. *Development*, *125*, 3015–25.

Hamidi, S., Nakaya, Y., Nagai, H., Alev, C., Kasukawa, T., Chhabra, S., Lee, R., Niwa, H., Warmflash, A., Shibata, T., & Sheng, G. (2020). Mesenchymal-epithelial transition regulates initiation of pluripotency exit before gastrulation. *Development*, *147*(3), dev184960.
URL https://doi.org/10.1242%2Fdev.184960

Han, L., Chaturvedi, P., Kishimoto, K., Koike, H., Nasr, T., Iwasawa, K., Giesbrecht, K., Witcher, P. C., Eicher, A., Haines, L., Lee, Y., Shannon, J. M., Morimoto, M., Wells, J. M., Takebe, T., & Zorn, A. M. (2019). Single cell transcriptomics reveals a signaling roadmap coordinating endoderm and mesoderm diversification during foregut organogenesis.
URL https://doi.org/10.1101%2F756825

Hashimoto, K., & Nakatsuji, N. (1989). Formation of the Primitive Streak and Mesoderm Cells in Mouse Embryos-Detailed Scanning Electron Microscopical Study. (primitive streak/cell migration/extracellular matrix/mouse gastrulation/scanning electron microscopy). *Development Growth and Differentiation*, *31*(3), 209–218.
URL https://doi.org/10.1111%2Fj.1440-169x.1989.00209.x

Hashmi, A., Tlili, S., Perrin, P., Martinez-Arias, A., & Lenne, P.-F. (2020). Cell-state transitions and collective cell movement generate an endoderm-like region in gastruloids.
URL https://doi.org/10.1101%2F2020.05.21.105551

Herrmann, B. (1991). Expression pattern of the Brachyury gene in whole-mount TWis/TWis mutant embryos. *Development*, *113*, 913–7.

Hiramatsu, R., Matsuoka, T., Kimura-Yoshida, C., Han, S.-W., Mochida, K., Adachi, T., Takayama, S., & Matsuo, I. (2013). External Mechanical Cues Trigger the Establishment of the Anterior-Posterior Axis in Early Mouse Embryos. *Developmental Cell*, *27*(2), 131–144.
URL https://doi.org/10.1016%2Fj.devcel.2013.09.026

Kanai-Azuma, M., Kanai, Y., Gad, J., Tajima, Y., Taya, C., Kurohmaru, M., Sanai, Y., Yonekawa, H., Yazaki, K., Tam, P., & Hayashi, Y. (2002). Depletion of definitive gut endoderm in Sox17-null mutant mice. *Development*, *129*, 2367–79.

Kubo, A., Shinozaki, K., Shannon, J., Kouskoff, V., Kennedy, M., Woo, S., Fehling, H., & Keller, G. (2004). Development of definitive endoderm from embryonic stem cells in culture. *Development*, *131*, 1651–62.

Kwon, G. S., Viotti, M., & Hadjantonakis, A.-K. (2008). The Endoderm of the Mouse Embryo Arises by Dynamic Widespread Intercalation of Embryonic and Extraembryonic Lineages. *Developmental Cell*, *15*(4), 509–520.
URL https://doi.org/10.1016%2Fj.devcel.2008.07.017

Lewis, S. L., & Tam, P. P. (2006). Definitive endoderm of the mouse embryo: Formation cell fates, and morphogenetic function. *Developmental Dynamics*, *235*(9), 2315–2329.
URL https://doi.org/10.1002%2Fdvdy.20846

Matsuo, I., & Hiramatsu, R. (2017). Mechanical perspectives on the anterior-posterior axis polarization of mouse implanted embryos. *Mechanisms of Development*, *144*, 62–70.
URL https://doi.org/10.1016%2Fj.mod.2016.09.002

McGrath, P., & Wells, J. (2015). SnapShot: GI tract development. *Cell*, *161*, 176–176.e1.

Monaghan, A., Kaestner, K., Grau, E., & Schütz, G. (1993). Postimplantation expression patterns indicate a role for the mouse forkhead/HNF-3 alpha, beta and gamma genes in determination of the definitive endoderm, chordamesoderm and neuroectoderm. *Development*, *119*, 567–78.

Mountford, P., Zevnik, B., Duwel, A., Nichols, J., Li, M., Dani, C., Robertson, M., Chambers, I., & Smith, A. (1994). Dicistronic targeting constructs: reporters and modifiers of mammalian gene expression. *Proceedings of the National Academy of Sciences*, *91*(10), 4303–4307.
URL https://doi.org/10.1073%2Fpnas.91.10.4303

Nowotschin, S., Hadjantonakis, A.-K., & Campbell, K. (2019a). The endoderm: a divergent cell lineage with many commonalities. *Development*, *146*(11), dev150920.
URL https://doi.org/10.1242%2Fdev.150920

Nowotschin, S., Setty, M., Kuo, Y.-Y., Liu, V., Garg, V., Sharma, R., Simon, C. S., Saiz, N., Gardner, R., Boutet, S. C., Church, D. M., Hoodless, P. A., Hadjantonakis, A.-K., & Pe'er, D. (2019b). The emergent landscape of the mouse gut endoderm at single-cell resolution. *Nature*, *569*(7756), 361–367.
URL https://doi.org/10.1038%2Fs41586-019-1127-1

Oppenheimer, J. M. (1940). The Non-Specificity of the Germ-Layers. *The Quarterly Review of Biology*, *15*(1), 1–27.
URL https://doi.org/10.1086%2F394599

Pander, C. H. (1817). *Dissertatio inauguralis sistens historiam metamorphoseos quam ovum incubatum prioribus quinque diebus subit.*. Typis Nitribitt,.
URL https://doi.org/10.5962%2Fbhl.title.48488

Peter, I., & Davidson, E. (2010). The endoderm gene regulatory network in sea urchin embryos up to mid-blastula stage. *Dev Biol*, *340*, 188–99.

Pfendler, K., Catuar, C., Meneses, J., & Pedersen, R. (2005). Overexpression of Nodal promotes differentiation of mouse embryonic stem cells into mesoderm and endoderm at the expense

of neuroectoderm formation. *Stem Cells Dev*, *14*, 162–72.

Pour, M., Kumar, A. S., Walther, M., Wittler, L., Meissner, A., & Nachman, I. (2019). Emergence and patterning dynamics of mouse definitive endoderm.
URL https://doi.org/10.1101%2F728642

Preibisch, S., Saalfeld, S., & Tomancak, P. (2009). Globally optimal stitching of tiled 3D microscopic image acquisitions. *Bioinformatics*, *25*(11), 1463–1465.
URL https://doi.org/10.1093%2Fbioinformatics%2Fbtp184

Rossi, G., Boni, A., Guiet, R., Girgin, M., Kelly, R. G., & Lutolf, M. P. (2019). Embryonic organoids recapitulate early heart organogenesis.
URL https://doi.org/10.1101%2F802181

Rueden, C., Schindelin, J., Hiner, M., DeZonia, B., Walter, A., Arena, E., & Eliceiri, K. (2017). ImageJ2: ImageJ for the next generation of scientific image data. *BMC Bioinformatics*, *18*, 529.

Sasaki, H., & Hogan, B. (1993). Differential expression of multiple fork head related genes during gastrulation and axial pattern formation in the mouse embryo. *Development*, *118*, 47–59.

Schindelin, J., Arganda-Carreras, I., Frise, E., Kaynig, V., Longair, M., Pietzsch, T., Preibisch, S., Rueden, C., Saalfeld, S., Schmid, B., Tinevez, J.-Y., White, D. J., Hartenstein, V., Eliceiri, K., Tomancak, P., & Cardona, A. (2012). Fiji: an open-source platform for biological-image analysis. *Nature Methods*, *9*(7), 676–682.
URL https://doi.org/10.1038%2Fnmeth.2019

Shahbazi, M. N., & Zernicka-Goetz, M. (2018). Deconstructing and reconstructing the mouse and human early embryo. *Nature Cell Biology*, *20*(8), 878–887.
URL https://doi.org/10.1038%2Fs41556-018-0144-x

Smith, L. (1985). Embryonic axis orientation in the mouse and its correlation with blastocyst relationships to the uterus. II. Relationships from 4 1/4 to 9 1/2 days. *J Embryol Exp Morphol*, *89*, 15–35.

Stower, M., & Srinivas, S. (2018). The Head's Tale: Anterior-Posterior Axis Formation in the Mouse Embryo. *Curr Top Dev Biol*, *128*, 365–390.

Sulston, J., Schierenberg, E., White, J., & Thomson, J. (1983). The embryonic cell lineage of the nematode Caenorhabditis elegans. *Dev Biol*, *100*, 64–119.

Tada, S., Era, T., Furusawa, C., Sakurai, H., Nishikawa, S., Kinoshita, M., Nakao, K., Chiba, T., & Nishikawa, S. (2005). Characterization of mesendoderm: a diverging point of the definitive endoderm and mesoderm in embryonic stem cell differentiation culture. *Development*, *132*, 4363–74.

Takaoka, K., & Hamada, H. (2012). Cell fate decisions and axis determination in the early mouse embryo. *Development*, *139*, 3–14.

Tam, P., & Behringer, R. (1997). Mouse gastrulation: the formation of a mammalian body plan. *Mech Dev*, *68*, 3–25.

Tam, P. P. L., & Loebel, D. A. F. (2007). Gene function in mouse embryogenesis: get set for gastrulation. *Nature Reviews Genetics*, *8*(5), 368–381.
URL https://doi.org/10.1038%2Fnrg2084

Toda, S., Blauch, L. R., Tang, S. K. Y., Morsut, L., & Lim, W. A. (2018). Programming self-organizing multicellular structures with synthetic cell-cell signaling. *Science*, (p. eaat0271).
URL https://doi.org/10.1126%2Fscience.aat0271

Turner, D., Baillie-Johnson, P., & Martinez, A. A. (2016). Organoids and the genetically encoded self-assembly of embryonic stem cells. *Bioessays*, *38*, 181–91.

Turner, D. A., Girgin, M., Alonso-Crisostomo, L., Trivedi, V., Baillie-Johnson, P., Glodowski, C. R., Hayward, P. C., Collignon, J., Gustavsen, C., Serup, P., Steventon, B., Lutolf, M. P., & Arias, A. M. (2017). Anteroposterior polarity and elongation in the absence of extra-embryonic tissues and of spatially localised signalling in gastruloids: mammalian embryonic organoids. *Development*, *144*(21), 3894–3906.
URL https://doi.org/10.1242%2Fdev.150391

van den Brink, S. C., Alemany, A., van Batenburg, V., Moris, N., Blotenburg, M., Vivié, J., Baillie-Johnson, P., Nichols, J., Sonnen, K. F., Arias, A. M., & van Oudenaarden, A. (2020). Single-cell and spatial transcriptomics reveal somitogenesis in gastruloids. *Nature*.
URL https://doi.org/10.1038%2Fs41586-020-2024-3

van den Brink, S. C., Baillie-Johnson, P., Balayo, T., Hadjantonakis, A.-K., Nowotschin, S., Turner, D. A., & Arias, A. M. (2014). Symmetry breaking germ layer specification and axial organisation in aggregates of mouse embryonic stem cells. *Development*, *141*(22), 4231–4242.
URL https://doi.org/10.1242%2Fdev.113001

Veenvliet, J. V., Bolondi, A., Kretzmer, H., Haut, L., Scholze-Wittler, M., Schifferl, D., Koch, F., Pustet, M., Heimann, S., Buschow, R., Wittler, L., Timmermann, B., Meissner, A., & Herrmann, B. G. (2020). Mouse embryonic stem cells self-organize into trunk-like structures with neural tube and somites.
URL https://doi.org/10.1101%2F2020.03.04.974949

Viotti, M., Nowotschin, S., & Hadjantonakis, A.-K. (2014). SOX17 links gut endoderm morphogenesis and germ layer segregation. *Nature Cell Biology*, *16*(12), 1146–1156.
URL https://doi.org/10.1038%2Fncb3070

Williams, M., Burdsal, C., Periasamy, A., Lewandoski, M., & Sutherland, A. (2011). Mouse primitive streak forms in situ by initiation of epithelial to mesenchymal transition without migration of a cell population. *Developmental Dynamics*, *241*(2), 270–283.
URL https://doi.org/10.1002%2Fdvdy.23711

Yamanaka, Y., Tamplin, O. J., Beckers, A., Gossler, A., & Rossant, J. (2007). Live Imaging and Genetic Analysis of Mouse Notochord Formation Reveals Regional Morphogenetic Mechanisms. *Developmental Cell*, *13*(6), 884–896.
URL https://doi.org/10.1016%2Fj.devcel.2007.10.016

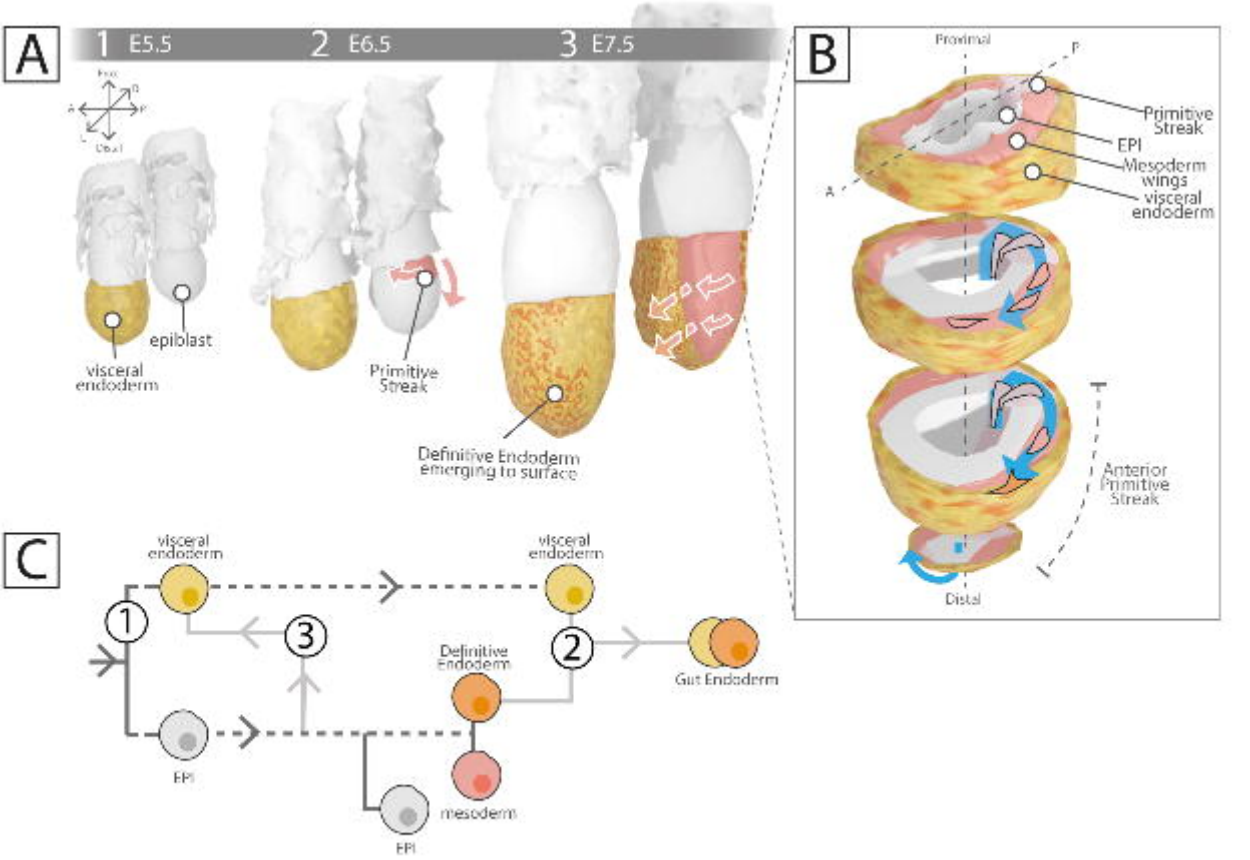
A
1 E5.5
2 E6.5
3 E7.5
epiblast
visceral endoderm
Primitive Streak
Definitive Endoderm emerging to surface
B
Proximal
Distal
Primitive Streak
EPI
Mesoderm wings
visceral endoderm
Anterior Primitive Streak
C
visceral endoderm
visceral endoderm
1
2
3
Definitive Endoderm
Gut Endoderm
EPI
mesoderm
EPI

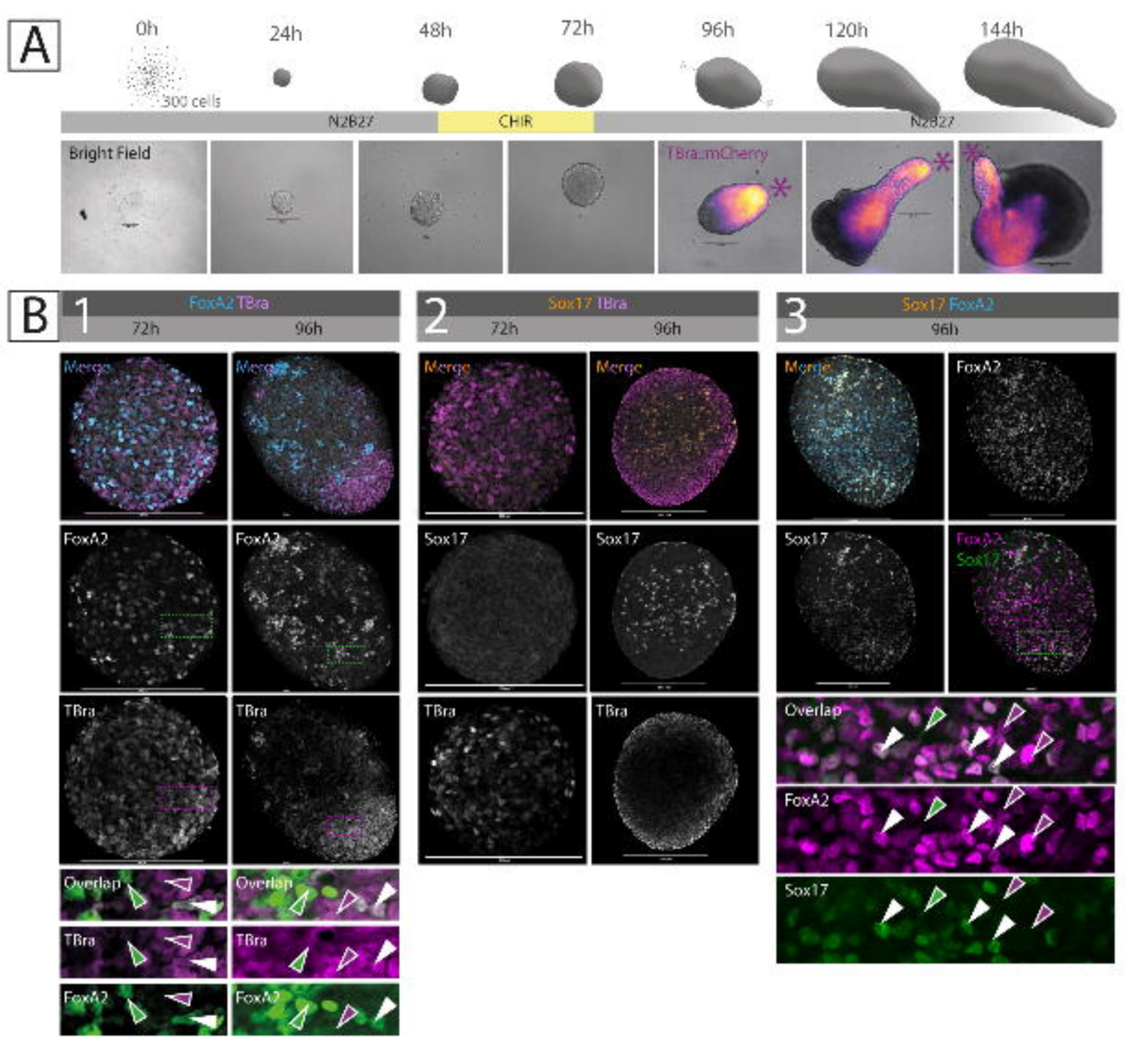
A
0h
24h
48h
72h
96h
120h
144h
300 cells
N2B27
CHIR
N2B27
Bright Field
TBra::mCherry
B
1
FoxA2 TBra
72h
96h
Merge
FoxA2
TBra
Overlap
2
Sox17 TBra
Sox17
3
Sox17 FoxA2
Sox17

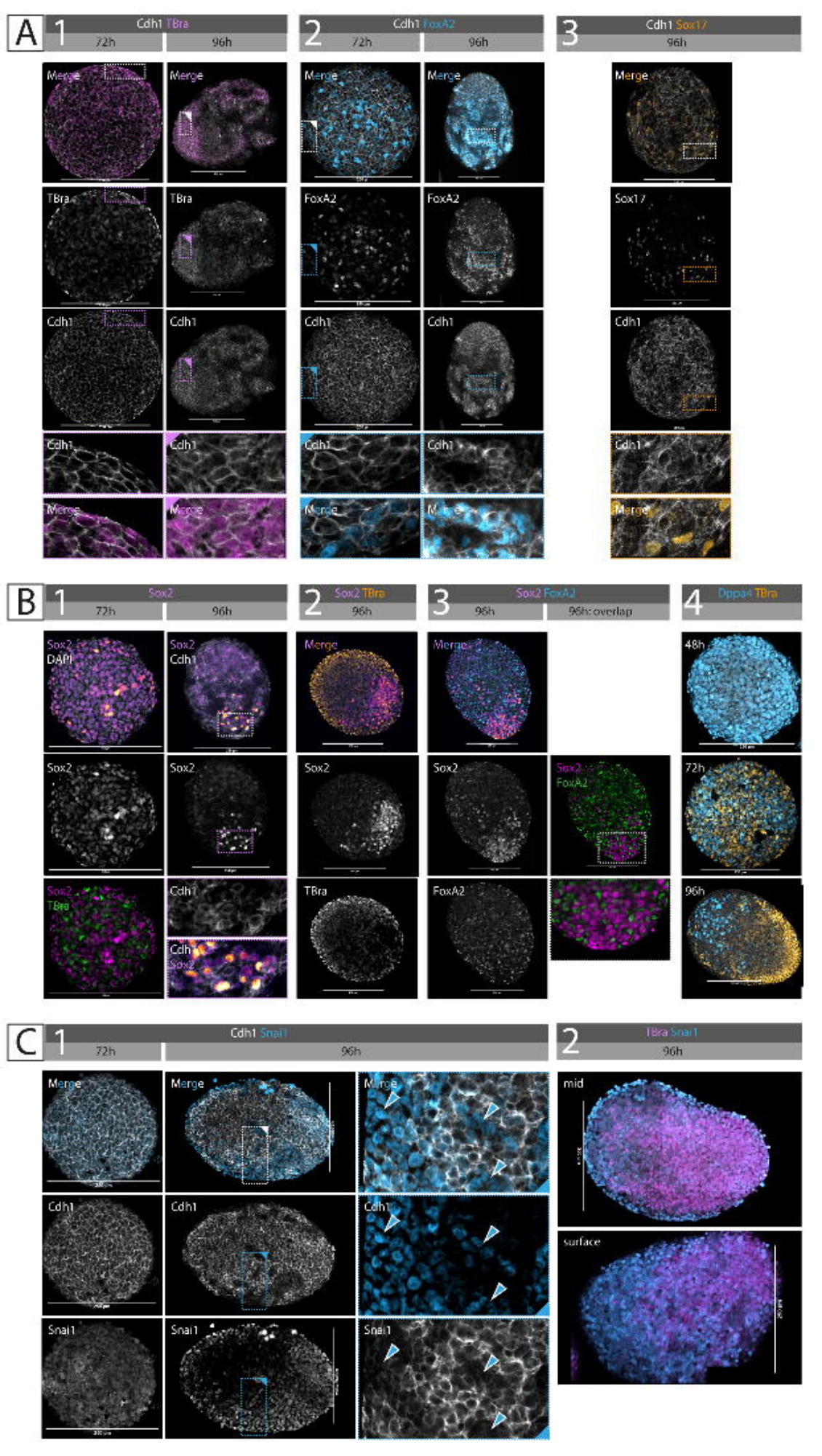
A
1
Cdh1 TBra
72h
96h
2
Cdh1 FoxA2
72h
96h
3
Cdh1 Sox17
96h
Merge
TBra
FoxA2
Sox17
Cdh1
B
1
Sox2
72h
96h
2
Sox2 TBra
96h
3
Sox2 FoxA2
96h
96h: overlap
4
Dppa4 TBra
DAPI
48h
72h
96h
C
1
Cdh1 Snai1
72h
96h
2
TBra Snai1
96h
Snai1
mid
surface

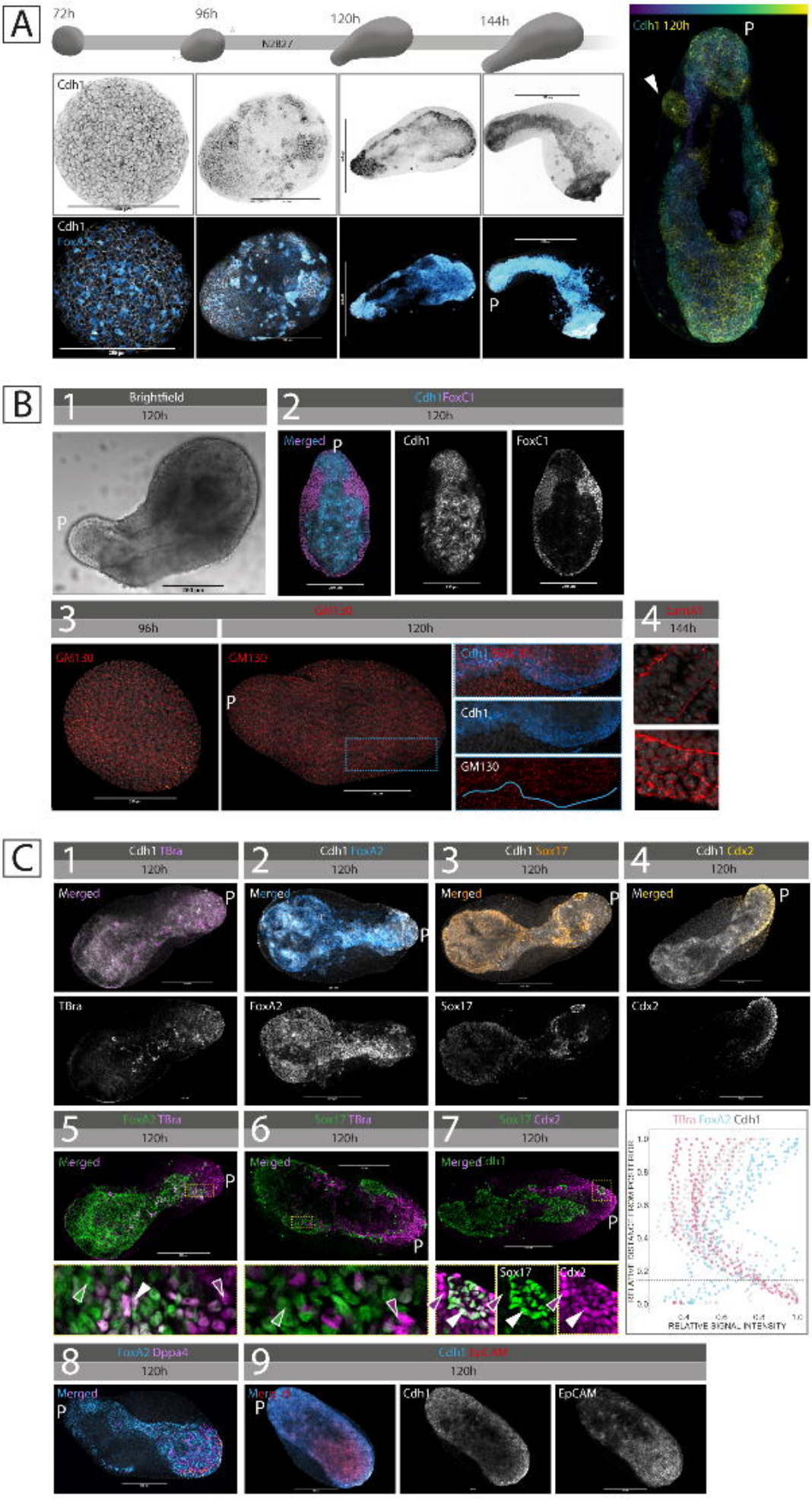
A
72h
96h
120h
144h
N2B27
Cdh1
Cdh1
FoxA2
P
Cdh1 120h
P
B
1
Brightfield
120h
P
2
Cdh1FoxC1
120h
Merged
P
Cdh1
FoxC1
3
GM130
96h
120h
GM130
GM130
P
Cdh1
GM130
4
GM130
144h
C
1
Cdh1 TBra
120h
Merged
P
TBra
2
Cdh1 FoxA2
120h
Merged
P
FoxA2
3
Cdh1 Sox17
120h
Merged
P
Sox17
4
Cdh1 Cdx2
120h
Merged
P
Cdx2
5
FoxA2 TBra
120h
Merged
P
6
Sox17 TBra
120h
Merged
P
7
Sox17 Cdx2
120h
Merged Cdh1
P
Sox17
Cdx2
TBra FoxA2 Cdh1
RELATIVE DISTANCE FROM POSTERIOR
RELATIVE SIGNAL INTENSITY
8
FoxA2 Dppa4
120h
Merged
P
9
Cdh1 EpCAM
120h
Merged
P
Cdh1
EpCAM

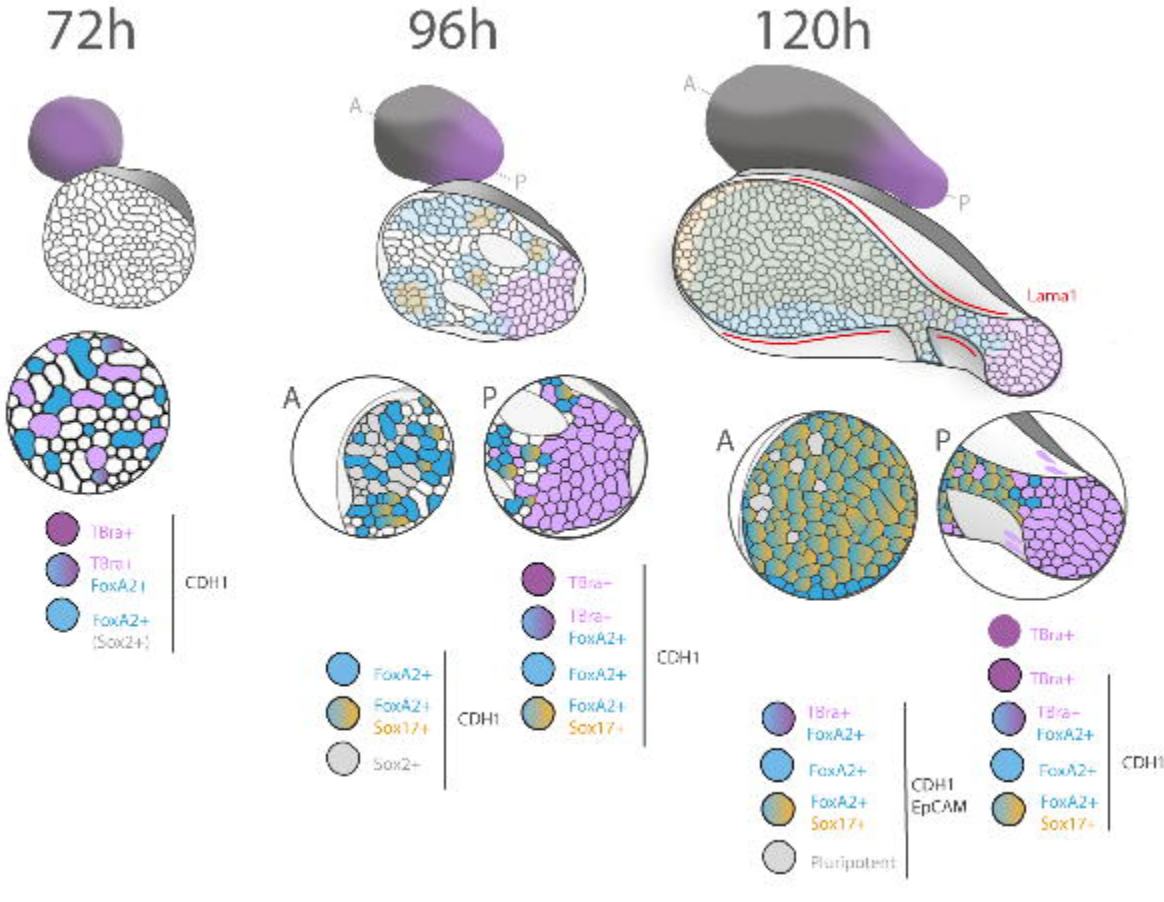
72h
96h
120h
A
P
Lama1
TBra+
TBra+
FoxA2+
FoxA2+
(Sox2+)
CDH1
FoxA2+
FoxA2+
Sox17+
Sox2+
CDH1
TBra+
TBra+
FoxA2+
FoxA2+
FoxA2+
Sox17+
CDH1
TBra+
FoxA2+
FoxA2+
FoxA2+
Sox17+
Pluripotent
CDH1
EpCAM
TBra+
TBra+
TBra+
FoxA2+
FoxA2+
FoxA2+
Sox17+
CDH1